Annu. Rev. Astron. Astrophys. 1993. 31: 717–61

X-RAY SPECTRA AND TIME VARIABILITY OF ACTIVE GALACTIC NUCLEI

Richard F. Mushotzky

Laboratory for High Energy Astrophysics, Code 666, Goddard Space Flight Center, Greenbelt, Maryland 20771

Christine Done and Kenneth A. Pounds

Department of Physics and Astronomy, Leicester University, University Road, Leicester LE1 7RH, England

KEY WORDS: quasars, Seyert galaxies, power spectra, radiation mechanisms

1. INTRODUCTION

The origin of the enormous luminosity seen in active galaxies such as quasars and Seyfert galaxies (AGN) is not understood. It is thought that this energy is liberated by the accretion of matter onto a massive black hole at the center of an otherwise normal galaxy (Rees 1984, Blandford & Rees 1992). One of the most important discoveries of the early days of X-ray astronomy (Elvis et al 1978) was that X-ray emission is an extremely common property of active galaxies and that much of the observed luminosity in AGN is radiated in the X-ray domain.

In fact, X-ray emission can be considered as a defining characteristic of the class of active galaxies. This is supported by X-ray survey results which find that, in the 2–10 keV band, there are more X-ray emitting Seyfert I galaxies per unit volume than found in surveys conducted in any other wavelength band (Danese et al 1986) and in the 0.2–2 keV band the surface density of X-ray discovered quasars is equal to or larger than that of optically discovered objects (Shanks et al 1991, Boyle et al 1993). In addition, the X-ray flux shows the fastest variability in any of the wave-

0066–4146/93/0915–0717$02.00

length ranges (see e.g. McHardy 1990) which indicates that it originates from a small region very close to the central object. Because of the large fraction of the luminosity that appears in the X-ray domain and its apparent association with the innermost regions of the black hole it is evident that detailed X-ray spectroscopy and timing observations will continue to have a crucial role in understanding the active galaxy phenomenon.

In order to limit this review we shall define active galactic nuclei (AGN) to include only Seyfert Is, Seyfert IIs and quasars, and will not, in general, discuss LINERs, BL Lac objects, nor OVV quasars [for a detailed definition of these terms and a description of the variety of AGN phenomena see Lawrence (1987) and Osterbrock & Mathews (1986)]. Briefly, we take Seyfert I galaxies (Seyfert 1943) to be objects that have a bright point-like nucleus in the optical and X-ray bands, have a "nonthermal" optical continuum, show broad ($\delta v \gtrsim 3{,}000$ km/sec) optical and UV permitted emission lines, and lie in recognizable galaxies. By contrast, Seyfert IIs have strong, narrow ($200 < \delta v < 2000$ km/sec) forbidden lines, little evidence for broad lines, and have very weak (if any) "nonthermal" optical-UV continua. To first order, quasars are more luminous examples of Seyfert Is, although the host galaxy is frequently much fainter than the central source and thus tends to be difficult to discern.

There is growing evidence that the apparently very different Seyfert Is and IIs are fundamentally the same. This view, based on current physical understanding of how the various types of AGN inter-relate is embodied in the so-called unification schemes. In the simplest versions, both radio-quiet quasars and Seyfert IIs are directly related to Seyfert Is, with the radio-quiet quasars being the higher luminosity objects (Schmidt & Green 1983) and with the nuclei of the Seyfert IIs being largely obscured from our direct line of sight by cold absorbing material (Antonucci 1993). The X-ray emission from Seyfert IIs supports these models, as they are typically much weaker in the soft X-ray band than the Seyfert Is, as expected if the innermost regions are obscured by absorbing material.

The radio-loud objects may, however, be intrinsically rather different from the radio-quiet ones. While the activity in both is probably powered by accretion onto a supermassive black hole, conditions in the radio-loud AGN apparently lead to the formation of a relativistic jet. Then the orientation of the observer with respect to the jet is the determining factor in the observed properties of these AGN (Padovani & Urry 1992). Viewed at angles close to the jet direction, the spectrum is dominated by the beamed emission. Relativistic time dilation effects and luminosity enhancement may lead to extreme variability, as seen in the optically violently variable objects (OVVs). The X-ray emission from these objects is also thought to arise from the jet, because radio-loud objects have rather

stronger X-ray emission and rather different X-ray spectra than radio-quiet objects (Worrall et al 1987, Zamorani et al 1981, Wilkes & Elvis 1987, Lawson et al 1992). In addition, the lack of X-ray spectral features at $E > 6$ keV (Kii et al 1992, Ohashi et al 1992) is thought to be due to jet related emission. Thus, to avoid the confusing effects of relativistic beaming, we will concentrate this discussion on radio-quiet AGN

We also define, for the purposes of the present review, the X-ray band to be from 0.1–100 keV. At lower energies (down to 13.6 eV for low redshift objects), absorption due to the interstellar medium of our galaxy makes observations of extra-galactic objects difficult, or impossible, while at higher energies the lack of sensitive instruments has severely curtailed the available data. This spectral range, nevertheless, corresponds (in decades of frequency covered) to the total EUV through IR bandpass. Given this large band, it is not surprising to find that a wide variety of different physical phenomena can arise, each dominating at different energies. For example, at energies less then 9.3 keV (the binding energy of the last K shell electron in Fe, the heaviest abundant element), the imprint of atomic processes, in both emission and absorption, are now being seen, while at higher energies Compton scattering and, perhaps, nuclear processes will be important. [For a summary of the physical mechanisms involved in X-ray spectra see Holt & McCray (1982).]

As noted above, two factors underline the importance of X-ray observations to the study of AGN. First, the X-ray emission is a major component of the total luminosity, being typically between 5 and 40% of the bolometric luminosity for AGN with $L(\mathrm{x}) < 10^{44}$ (Ward et al 1987). Second, the X-ray band is the only spectral region in which large amplitude ($\delta I/I \sim 1$), rapid ($\Delta T < 1$ day) variability is common in radio-quiet objects (McHardy 1988, Pounds & McHardy 1988). Even shorter timescales are evident in some objects, with the most rapid variability being on the order of minutes (Lawrence et al 1985, Kunieda et al 1990). It is this combination of large luminosity and rapid variability of the X-ray emission that provides the strongest support to date for the identification of the central object with an accreting black hole (Guilbert et al 1983).

2. BRIEF HISTORY OF X-RAY OBSERVATIONS OF AGN

The first successful X-ray observations of an AGN were performed in the 1960s with rocket and balloon experiments which detected emission from the bright quasar, 3C273 (Bowyer et al 1970). The third *Uhuru* catalog, the first large assembly of X-ray sources (Giacconi et al 1974), identified X-ray emission from the 3 brightest AGN in the X-ray sky (3C273, NGC

4151, and Cen-A), only one of which, NGC 4151, is classified as a Seyfert I galaxy. The ubiquity of X-ray emission from Seyfert I galaxies (Elvis et al 1978) was established by the first catalog from the *Ariel-V* sky survey (Cooke et al 1978). At the same time the first X-ray spectral results for the brightest AGN were published from *OSO-7* and *Uhuru* data (Tucker et al 1973, Winkler & White 1975, Mushotzky et al 1976). Early measurements of X-ray variability were obtained from the *OSO-7* and *Copernicus* satellites (Winkler & White 1975, Davidson et al 1975), while the *Ariel-V* survey indicated that X-ray variability on timescales greater than one day was a rather common property of AGN (Marshall et al 1981).

Improved (although still crude) X-ray spectra of NGC 4151 and Cen-A, from *OSO-8* (Mushotzky 1978a,b) and *Ariel-V* (Ives et al 1976, Stark et al 1977, Barr et al 1977), established the power-law shape of the X-ray continuum, measured a significant low energy roll-over attributable to photoelectric absorption by a column density more than 10^{22} atoms cm^2, and detected 6.4 keV Fe line emission in both objects. The first large spectral samples of AGN, obtained with the *HEAO-1* satellite (Mushotzky et al 1980, Mushotzky 1982, Rothschild et al 1983, Mushotzky 1984), were well modeled by a power law in the 2–20 keV band, with little intrinsic absorption, and the observed range in photon spectral index was narrowly distributed around 1.7 (Figure 1). This mission also performed the first extended and sensitive search for variability (Tennant & Mushotzky 1983), finding very few objects that exhibited rapid (< a few hours), large amplitude (factor of 2) changes.

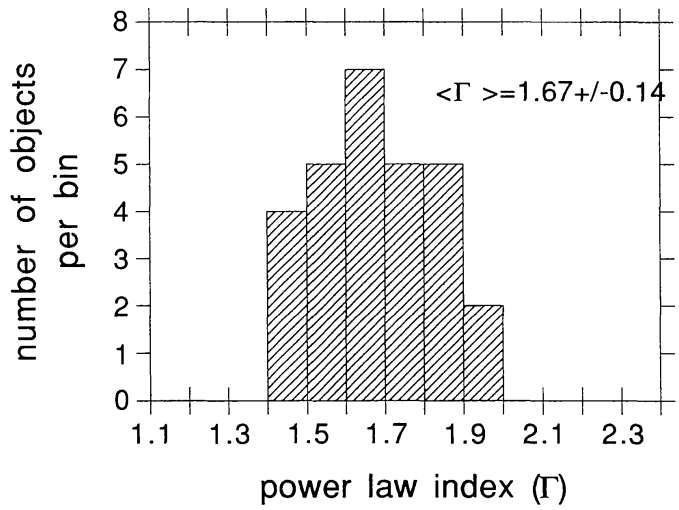

Figure 1 Distribution of photon spectral indices from power-law fits to the *Ginga* data for 28 active galaxies. The data were obtained from Nandra (1991) and Awaki (1991). The median spectra index is $\Gamma = 1.67$, in good agreement with previous results.

The *HEAO-2* satellite (alias the *Einstein Observatory* or *EO*), by using focusing X-ray optics, improved on the sensitivity of the *HEAO-1* experiments by a factor of >100 for source detection and increased the number of known X-ray emitting AGN by more than an order of magnitude. These data demonstrated that AGN of all types are powerful X-ray emitters (Zamorani et al 1981) and that X-ray observations could detect AGN out to quite high redshifts (Tananbaum et al 1979). The *EO* imaging proportional counter (IPC) obtained X-ray fluxes for ~ 1000 AGN, and the *EO* solid state spectrometer (SSS) gave the first higher quality spectra of AGN, the latter confirming the narrow distribution of spectral slopes around 1.7 in the 0.7–4 keV band. However, some of the lower luminosity Seyferts in this sample were not well described by a simple power law with absorption by cold material, but required a more complex fit (Reichert et al 1985, Petre et al 1984). The variety of low energy spectra was also underlined by data from a larger sample of low resolution AGN spectra, from the *EO* IPC, covering the softer 0.2–4.5 keV band. In this band simple power-law fits to the IPC spectra showed a wide range of slopes (Wilkes & Elvis 1987), contrasting with the apparent uniformity of the spectra in the 2–20 keV band.

EXOSAT, launched in 1983, provided the first detailed temporal studies of a large sample of Seyfert galaxies. Its highly eccentric orbit allowed continuous observations of up to three days. From these data the first power density spectra were derived, showing that the variability was stochastic, with no characteristic timescale (Lawrence et al 1987, McHardy & Czerny 1987). The *EXOSAT* observations showed that rapid, large amplitude variability was indeed a common feature of Seyfert galaxies (McHardy 1990, Pounds & McHardy 1988), contrasting with the earlier *HEAO-1* results. The broad energy coverage of *EXOSAT* also resulted in the discovery that a sharp rise at low energy, the so-called soft excess (Arnaud et al 1985), occurs in the spectra of $\sim 50\%$ of Seyfert galaxies (Turner & Pounds 1989). The increased sample of AGN spectra obtained by *EXOSAT*, furthermore, confirmed the *HEAO-1* result of the uniformity of the 2–20 keV power-law index in Seyfert galaxies (Turner & Pounds 1989).

The *Ginga* Large Area Counter (LAC), launched in 1987, provided a substantial further increase in the sensitivity of (proportional counter) low resolution X-ray spectroscopy in the 2–20 keV band. In particular, *Ginga* data allowed detailed spectral decomposition to be performed for the first time, showing that a significant fraction of all Seyfert galaxies exhibit Fe 6.4 keV lines (Pounds et al 1989, 1990, Matsuoka et al 1990, Nandra 1991), and at a level that is much more intense than can be explained by the generally small columns of absorbing material in the line of sight (Inoue

1990). These *Ginga* AGN data also showed a spectral flattening at $E > 8$ keV which could most readily be attributed to the reprocessing of a (substantial) fraction of the incident X-ray flux by cold material near the central engine, either totally or partially out of the line of sight (Lightman & White 1988, Guilbert & Rees 1988). Other *Ginga* observations allowed the first crude spectra of a significant sample of quasars in the 2–20 keV band (Williams et al 1992) to complement the *EO* lower energy data.

The most recent X-ray data on AGN have come from *ROSAT* and BBXRT. The *ROSAT* all-sky survey (RASS), performed in 1990, has dramatically increased the samples of X-ray-selected AGN available for study in the 0.1–2 keV band. It is anticipated that at least 50% of the more than 60,000 RASS sources will turn out to be previously unknown AGN. Pointed *ROSAT* observations of individual AGN are beginning to provide high signal-to-noise, albeit low resolution, soft X-ray spectra. These data are complemented by results from BBXRT, flown on the U.S. Space Shuttle in 1990, which provided moderate resolution, broadband spectra for a small, but significant sample of AGN.

Naturally, much of the progress in this field has come from improvements in instrumentation [for a history of X-ray astronomy instrumentation we refer the reader to Bradt et al (1992)]. The sealed proportional counters responsible for virtually all current 2–20 keV spectra had spatial resolutions of $>1^\circ$ and an energy resolution of $\sim 18\%$ at 6 keV. At lower energies, the *EO* proportional counter and the *EXOSAT* low energy counters had spatial resolutions of $>10''$ and energy resolution of $\sim 100\%$ at 1 keV, while the SSS on the *EO* had a resolution of $\sim 16\%$ at 1 keV. In this review, we refer to the proportional counter spectra as having "low resolution" and the solid state device data as having "moderate resolution." The limited energy resolution and/or bandwidth of most X-ray detectors used to date (typically only 4–20 spectral resolution elements in a given detector), requires modeling of the spectrum in order to derive detailed spectral parameters. Thus, it is usually not possible to directly determine the form of the continuum or line properties; instead it is necessary to develop a model and fit it to the data. This is a fundamental difference between current X-ray and optical spectroscopy. Only very recently have some data become available for only a few AGN, from BBXRT and combined *ROSAT*/*Ginga* observations, that have allowed fits over the 0.3–12 keV band, with sufficient spectral elements to allow reasonably unambiguous modeling of both hard and soft X-ray components.

At the time of writing (1992) we are in the midst of a significant enhancement in observational capabilities. The *ROSAT* satellite (Trümper 1990) has improved sensitivity, angular resolution, and energy resolution compared with the *EO*, and promises a large increase in the number of AGN

with high-signal-to noise observations. *ASCA* (Inoue 1992), to be launched in 1993, has an energy resolution of 2–5% at 6 keV and 10% at 1 keV and should greatly increase the number of broadband, high signal-to-noise, moderate resolution spectra. We thus expect a rich harvest of new X-ray data from AGN over the next 3–4 years.

3. SPECTRAL FORM

3.1 *Overview*

To first order, the 2–50 keV spectrum of the great majority of Seyfert I galaxies can be characterized by a simple power law of form $F(E) = AE^{-\Gamma}$ ph/cm^2/sec/keV. In this sense the X-ray spectra are continuum dominated. The strongest broad spectral feature in the 0.1–100 keV energy range is low energy absorption due to photoelectric absorption of cold or partly ionized material in the line of sight to the nucleus. Our galaxy tends to have column densities at high galactic latitude of order $\sim 3 \times 10^{20}$ atoms/cm^2, which modifies the X-ray spectrum primarily at $E < 0.6$ keV. Uncertainty in the exact value of the galactic column, whether in our own galaxy or intrinsic to the AGN, can consequently have a strong influence on the perceived form of the low energy emission spectrum.

Until recently the best signal-to-noise X-ray spectra were of relatively low resolution and thus only the strongest features could be seen (Elvis et al 1987). Iron is the most abundant heavy element and its large absorption cross section at high energy, combined with a high fluorescent yield, indicates that the strongest spectral features at $E > 6$ keV should be due to Fe. These include Fe fluorescent emission at 6.4 keV—the only strong spectral line from near-neutral (or cold) material, He-like and H-like lines at 6.67 and 6.97 keV from ionized material, and K absorption edges between 7.1 and 9.3 keV, depending on the ionization state of the material. In the 0.5–3 keV band, spectral features due to the K shell transitions of O, Mg, Si, and S, and L shell transitions of Fe may occur. However, since these elements have low fluorescent yields, the strongest spectral features at low energy from cold material are likely to be due to absorption. Highly ionized material, in contrast, can have both emission and absorption features across the entire X-ray spectral band (Krolik & Kallman 1987). The strongest features in both emission and absorption at $E < 2$ keV (Krolik et al 1985) are expected to be due to oxygen K and Fe L shell transitions.

3.2 *Spectra of Seyfert Is*

3.2.1 CONTINUUM Simple fits to power-law spectra over the 2–20 keV band give photon number indices (Mushotzky 1984, Halpern 1982, Turner

& Pounds 1989, Awaki 1991 et al, Nandra 1991) that are narrowly distributed around 1.7, with a 1 σ width of 0.13 which is believed to represent a true dispersion in spectral slopes around the mean. Broad line radio galaxies (BLRGs) show the same X-ray spectral shape as Seyfert Is (Mushotzky 1984) in this band. The extension of this power law to $E > 50$ keV is based on only on a few objects (Cen-A: Baity et al 1981, NGC 4151: Baity et al 1984, and 3C273: Primini et al 1979) and the sum of 10 other, fainter, Seyfert Is (Rothschild et al 1983).

Indeed, the spectrum of NGC 4151 has been observed to steepen at $E \sim 50$ keV (Baity et al 1984, Jourdain et al 1992) and we note that a value of $\Gamma = 1.7$ would yield a total luminosity diverging with energy, as $E^{1/3}$; hence a cutoff must exist. If this cutoff has energy $E_{(\max)}$ then the total amount of energy goes as $E_{(\max)}^{(2-\Gamma)}/(2-\Gamma)$ and thus is quite sensitive to the slope of the continuum. However, it is now thought (see next section) that this mean spectral index may not represent the true spectrum of the source; rather it appears to be an average of a steeper intrinsic spectrum, of $\Gamma \sim 2.0$, and an additional, flatter component which is apparently produced as a result of reprocessing in material close to the central source.

The spectrum of the X-ray background (XRB) provides an integral constraint on the total flux from AGN. Since it is thought that AGN make up most of the XRB, the spectrum of the average AGN must steepen at energies above 60 keV in the observer's frame (Rothschild et al 1983) in order not to exceed the background flux. Using $\Gamma = 2.0$ (see Section 2.3 below) and $E_{(\max)}$ of 60 keV, the AGN X-ray luminosity is reduced by a factor of 8 compared to $\Gamma = 1.7$ and $E_{(\max)} = 2$ MeV. Higher signal-to-noise spectra of a significant sample of AGN at $E > 50$ keV are obviously necessary to settle this issue.

3.2.2 FE K EMISSION LINES Deep *Ginga* observations (Pounds et al 1989, 1990; Matsuoka et al 1990; Awaki et al 1991; Nandra et al 1991) have shown that Fe line emission at $\sim$6.4 keV, which is attributed to fluorescence of cold material, is a common property of Seyfert Is. The distribution in equivalent widths (EWs) seen in Seyfert 1 galaxies is apparently quite broad, with $50 < \mathrm{EW} < 350$ eV (Figure 2), but the errors are rather large (Nandra 1991, Awaki et al 1991). Significantly, there is no apparent correlation of line strength with line-of-sight column density. The mean line energy, $\langle E \rangle = 6.4$ keV, is consistent with fluorescence from cold material with rather low velocity (Nandra 1991, Awaki 1991); generally, a line at 6.7 keV, as expected from thermal emission, can be excluded (Figure 3). For $\sim$20% of the Seyferts the data are significantly better described by a broad line of $\sigma \sim 0.7$ keV, and a line this broad cannot be excluded in any of the *Ginga* Seyferts (Nandra 1991).

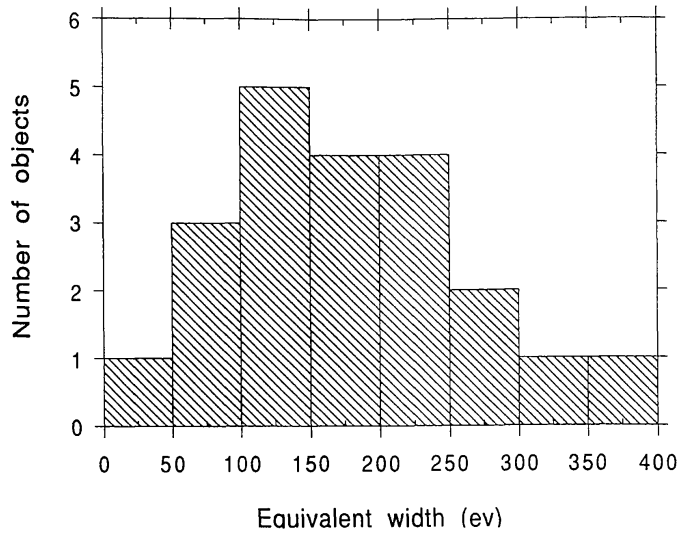

Figure 2 Distribution of of Fe line equivalent widths from *Ginga* observations of 21 AGN. The data were obtained from Nandra (1991) and Awaki (1991). Only positive detections are included.

The three BLRGs with high quality spectra [3C382 (Kaastra et al 1991), 3C390.3 (Awaki 1991), and 3C445 (Pounds 1990)] also show Fe K lines; 3C445 also shows a high X-ray column density.

If the line does indeed arise from fluorescence from cold material, then its strength indicates that a significant fraction of the solid angle visible to the continuum source must be filled with material of column density $> 10^{22.5}$ atoms/cm^2 (Makishima 1986, Matt et al 1991, George & Fabian 1991); this is in contrast to the general lack of absorbing material along the line of sight to these sources (Pounds et al 1989). Thus, the discovery of frequent strong Fe line emission from Seyfert Is with little or no line-of-sight absorbing gas was a surprise.

The principal exception to this is NGC 4151 (coincidentally one of the X-ray-brightest AGN), where the large column density inferred from the low energy roll-over in the spectrum can produce the observed line, provided iron is overabundant by a factor of 2 (Yaqoob & Warwick 1991). This conclusion is supported by a BBXRT high resolution spectrum of NGC 4151 (Weaver et al 1992) which shows that the main component of the 6.4 keV line is at the redshift of the galaxy and is narrow, with FWHM < 7500 km/sec. A weak indication of a broad component to the line, of FWHM $\sim$ 30,000 km/sec, from both the BBXRT (Weaver et al 1992) and *Ginga* data (Yaqoob & Warwick 1991), suggests a possible secondary source of line production.

3.2.3 OTHER DISTORTIONS AT $E > 6$ keV In addition to the Fe Kα line there are also other significant deviations from a power law at >6 keV in many

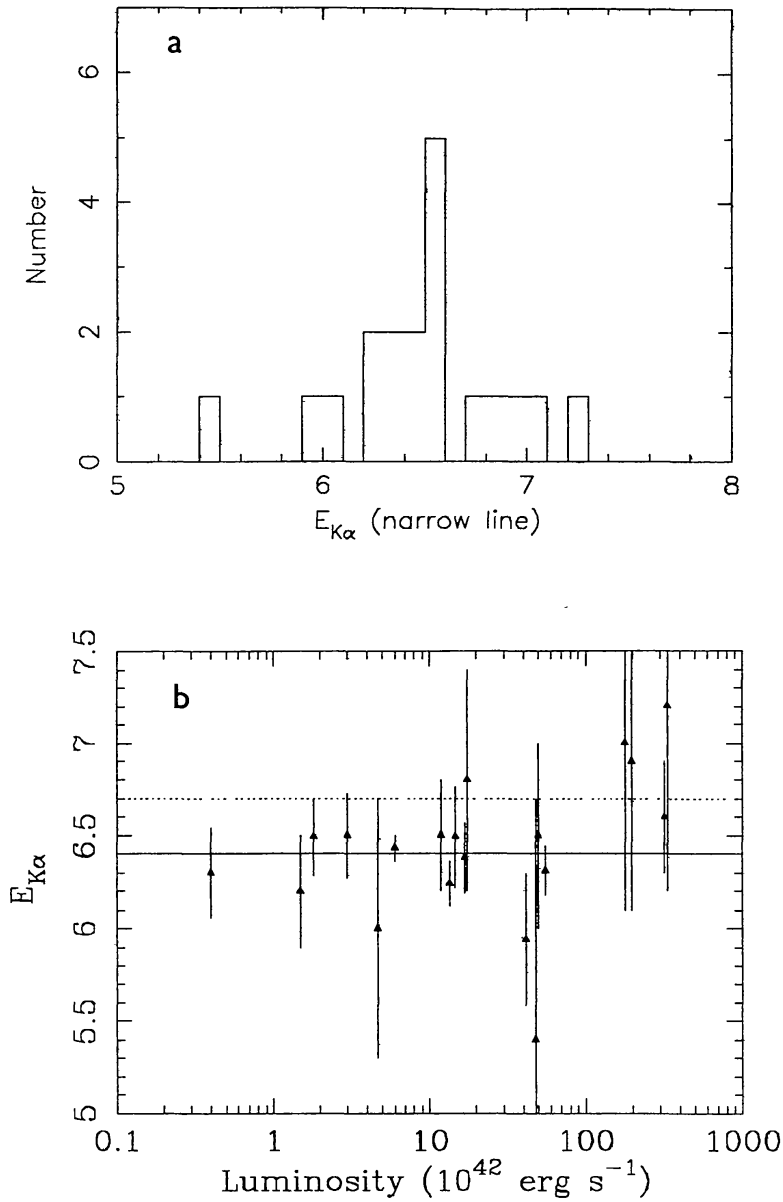

Figure 3 (*a*) Distribution of Fe line energies in the rest frame of the AGN. Notice the strong clustering around 6.4 keV. The data were obtained from Nandra (1991). (*b*) Fe K line energy versus X-ray luminosity. The solid line is drawn at 6.4 keV as appropriate for fluorescence from cold material while the dotted line is drawn at 6.7 keV as appropriate from recombination or fluorescence of ionized material. $L(x) < 10^{44}$ ergs/sec the data are consistent with $E = 6.4$ keV. (From Nandra 1991.)

Seyfert I galaxies. Co-adding 12 separate *Ginga* AGN spectra of 9 AGN to increase the signal-to-noise (the so-called *Ginga*-12 sample), Pounds et al (1990) found that, in addition to the Fe K line, there was a decrement between 7–8 keV and a flattening of the spectrum at higher energies (see Figure 4*a*). This flattening at higher energies has since been seen in

individual objects with high signal-to-noise, such as IC4329A (Piro et al 1990), and appears to be relatively common in Seyfert Is (Nandra 1991). The mean flattening in spectral index between 2–10 and 10–18 keV is $\delta\Gamma \sim 0.5$ (Nandra 1991). The fitted edge energy is strongly convolved with the Fe K line and the spectral flattening in the analysis of low resolution proportional counter spectra. However, for simple fits, including power-law, line, and edge, it appears that a significant fraction of Seyfert Is are better described by an edge from ionized rather than cold (near-neutral) iron (Nandra 1991).

Possible interpretations The Fe K line and "hard tail" features are consistent with the idea that the primary X rays are reprocessed (or "reflected") in optically thick material subtending a substantial solid angle to the X-ray source (Lightman & White 1988, Guilbert & Rees 1988, George & Fabian 1991, Matt et al 1991), possibly the putative accretion disk. The reflection albedo is energy dependent, as at low energies, $E < 2$ keV, there are many elements (C, N, O) that will photoelectrically absorb any incident flux, so few photons are reflected. However, the albedo increases at higher energies due to the decreasing abundance of the higher Z elements required for photoelectric absorption. Iron is the last abundant element that can significantly affect the probability of reflection, leading to a marked "pseudo-absorption feature" in the reflected flux from 7.1–9 keV, together with the associated Fe Kα fluorescence line with a predicted equivalent width of ~ 150 eV. At higher energies, Compton down-scattering and the reduction of the scattering cross-section deplete the number of photons reflected, resulting in a broadband spectral bump, peaking at ~ 20–30 keV.

Thus reflection from material out of the line of sight provides a self-consistent explanation for the Fe Kα line, some of the decrement at ~ 8 keV (but see also the section on ionized absorption below), and the high energy excess. This so-called *Compton reflection* model introduces four new free parameters into a spectral fit: the fraction of all photons that are reflected by the scatterer [essentially the solid angle covered by the scatterer ($\Omega/4\pi$)], the inclination of the scatterer to the line of sight, the element abundance, and the ionization state of the material. Figure 4*b* shows the Compton reflection model used in the fit to the *Ginga*-12 spectrum. This spectrum is now adequately fit, with a steeper intrinsic power-law spectrum, of $\Gamma = 1.9$ rather than 1.7, and a solid angle indicating $\Omega/2\pi = 1.5$ (i.e. indicative of a flared disk) viewed close to face on, with iron at twice solar abundance (Pounds et al 1990).

For a larger *Ginga* sample of Seyfert I galaxies, albeit with individual errors that are relatively large, Nandra (1991) finds a distribution of covering fractions of the material with a mean value of $\Omega/2\pi \sim 1$, again

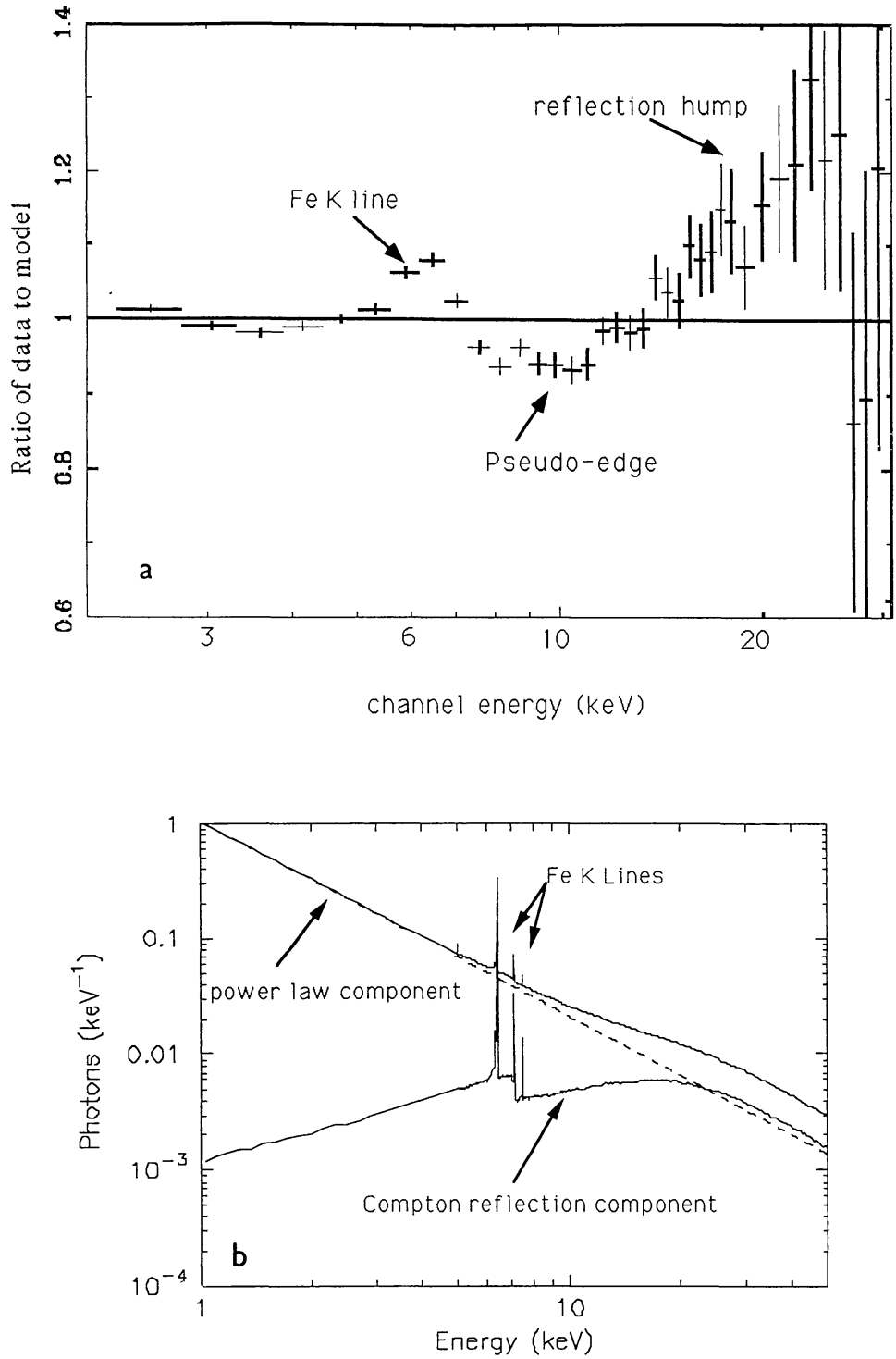

Figure 4 (*a*) The ratio of the *Ginga*-12 data to a simple power-law model. Note the deviations at ~6 keV, 8 keV, and $E > 10$ keV which can be interpreted in the Compton reflection model as the Fe K line, a pseudo-edge, and the reflection hump. In this ratio diagram the relative intensity of the features can be read off directly, e.g. the strength of the Fe K line is ~150 eV equivalent width (Pounds et al 1990). (*b*) The theoretical distribution of flux from a Compton reflection model (George & Fabian 1991).

with a steep intrinsic power law of mean index 1.9. If the $\Gamma = 1.7$ spectral form is indeed a conspiracy formed by the summation of a 1.9 index and a Compton reflection component, the narrow distribution in observed index implies a strong coupling between the intrinsic index and the fraction of solid angle occupied by the reflector. This could be a selection effect where, for example, most of the Seyfert Is are observed at relatively small inclinations, consistent with the unified models (see Antonucci 1993 in this volume).

Such geometrical selection effects can be tested by measurement of the Fe K line profile. If the material is in the form of an accretion disk, Doppler and gravitational broadening will combine to produce a characteristic skewed line profile (Fabian et al 1989; George & Fabian 1991; Matt et al 1991, 1992; Laor 1991), where the detailed line shape depends on inclination and the emissivity law of the disk. Typically such a line will be broad, with a Gaussian width of at least several hundred eV. In principle measurement of such a line profile can determine the distance of the line emitting region from the central object, in units of the Schwarzschild radius, and thus "prove" the existence of a compact, massive object. Except for NGC 4151, where the observation of a narrow (<300 eV FWHM) line (Weaver et al 1992) supports an origin in the line-of-sight (nondisk) cold material, the data so far do not usefully constrain these models. Similarly, an absorption edge in the reflected spectrum may be considerably distorted by these effects (Matt et al 1991), but again higher resolution data than presently available are required to see this.

An alternative explanation proposed for the observed Fe K-edge and high energy excess invokes *partial covering* of the X-ray source by cold, dense material, an idea first suggested to explain the "soft excess" in NGC 4151 (Holt et al 1980). In this scheme a fraction (which may be as much as $\sim 98\%$) of the photons seen by the observer are absorbed by quite thick [$N(\mathrm{H}) > 10^{23}$ atoms/cm^2] material (Matsuoka et al 1990, Piro et al 1990), while the rest are relatively unaffected by such absorption. The large column is essentially opaque below ~ 6 keV, so that a simple power-law fit to the overall spectrum has an apparent excess above this energy. The large column density material will also produce an iron edge in the total spectrum, whose optical depth is considerably greater than that predicted by the low energy absorption. As the covering material is optically thin to Thomson scattering, reflection should be weak, but, since the cross-section for producing the Fe line is larger than the electron scattering cross-section, the material can efficiently produce line emission. The amount of line emission predicted in these models has not been calculated in detail, however (Inoue 1990). The theoretical justification for this model has been provided in the "chaotic" central region model of Ferland & Rees (1988).

While the partial covering model provides a good analytic fit to some *Ginga* AGN spectral data, the particular values of column density and covering fraction derived have no obvious physical justification and thus this model is somewhat less physically appealing than reflection from an accretion disk. However, recent models of spherical accretion (Sivron & Tsuruta 1993) have recently been derived that may provide a physical basis for these values.

As the reflection and partial covering models have slightly different spectral shapes they can in principle be distinguished. However, even with *Ginga* data the typical signal-to-noise ratios of most AGN spectra do not allow a definitive test (e.g. Piro et al 1990). It is interesting to note that the (considerably brighter) Galactic black hole candidate (Section 6.4), Cyg X-1, is better fit by reflection than partial covering (Done et al 1992a).

However, there are a few Seyferts where the X-ray spectrum is better fit by partial covering rather than by simple reflection models, in particular MCG-5-23-16 (Piro et al 1991) and NGC 6814 (Turner et al 1992, Yamauchi et al 1992). Also, some AGN spectra, although well described by reflection at high energies, show variable absorption at low energies, suggesting partial covering of the X-ray source by a lower column than that required to produce the high energy excess (e.g. NGC 5506: Bond et al 1992). Still other AGN require only this lower column partial covering without substantial reflection (NGC 4151: Yaqoob et al 1993, Cen-A: Maisack et al 1992).

In summary, it is not clear what fraction of all AGN are better described by partial covering or simple power-law models, rather than the widely used Compton reflector model, or even if these models are mutually exclusive. It may well be that the objects best fit by the partial covering model are related to Seyfert II galaxies (see Section 3.4 below).

3.2.4 EXCESS EMISSION BELOW 2 keV Emission above that expected from a simple power law, the so-called soft excess, occurs in at least 30% of all hard-X-ray-selected AGN (Turner & Pounds 1989). Broad-band *HEAO-1* data (Singh et al 1985), *EXOSAT* results (Arnaud et al 1985, Turner & Pounds 1989), *Einstein* IPC and SSS spectra of Seyfert I galaxies (Kruper et al 1990, Turner et al 1991), BBXRT spectra (Turner et al 1993a), and recent *ROSAT* and *Ginga* results (Pounds et al 1993) all indicate that the observed spectra frequently steepen at $E < 2$ keV. The more recent data show that this steepening can be rather abrupt and that the soft spectral component generally does not "contaminate" the higher energy data. The soft emission component has typically been modeled with a black body of temperature < 150 eV (Urry et al 1989), a steep power law of photon index > 3 (Turner & Pounds 1989), or by a thermal bremmstrahlung spectrum of $kT < 500$ eV.

The form of the soft excess does not exhibit a uniform pattern (Turner et al 1991) and it appears likely that a variety of phenomena are occurring (Mushotzky 1991, Turner et al 1991). In particular, some objects are better fit by line-like features than a steep continuum, while other AGN show both. Given the poor spectral resolution of most detectors in this energy band, only the very strongest line features can be seen (Elvis & Lawrence 1988). The first reports of soft X-ray line emission line came from *EO* SSS observations (Petre et al 1984, Turner et al 1991) showing features at $E \sim 0.8$ keV, with ~ 100 eV EW, which were interpreted as Fe L emission lines or to the OVIII Lyman limit in emission (Netzer 1993). Recent *ROSAT* observations of several Seyferts (Turner et al 1993b) have claimed detection of similar features. The presence of spectral features can substantially modify the apparent shape of the spectrum in a low resolution detector, like the *EO* IPC or *ROSAT* PSPC (Position Sensitive Proportional Counter), if not fit explicitly, (Section 3.1) and thus considerable caution must be exercised in interpreting simple power-law fits to these data.

Possible interpretations A possible explanation for the continuum soft excess is thermal emission from the hot, innermost region of the accretion disk (Arnaud et al 1985, Pounds et al 1986, Czerny & Elvis 1987). However, it is difficult to explain the breadth of the disk emission spectrum (which is proposed to extend from the optical/UV to the soft X rays) without requiring super-Eddington luminosities in simple optically thick, geometrically thin, Shakura-Sunyaev models (Bechtold et al 1987). Several authors have suggested that inclusion of the vertical transfer of radiation (including Compton scattering) and general relativistic effects (Czerny & Elvis 1987, Wandel & Petrosian 1988, Sun & Malkan 1989, Laor & Netzer 1989) may make these models viable. Recent steps in this direction (Laor 1990, Ross et al 1992) look promising.

However, the production of the UV/soft X-ray luminosity entirely by viscous dissipation in a thin accretion disk is seriously at odds with the observed pattern of variability seen in both NGC 5548 and NGC 4151 (see Section 6.3) . Here the near simultaneity of changes in the UV lines and continuum and in the X-ray band can best be explained in the context of an X-ray illuminated accretion disk (Collin-Souffrin 1992, Ross & Fabian 1992), consistent with the reflection model interpretation of the hard X-ray spectral features. In this view some $\sim 10\%$ of the energy incident on the disk or any other cold material near the central engine is reflected, the remainder being thermalized, producing a broad spectrum, in which intensity changes propagate at the speed of light. The X-ray illumination also creates a hot, ionized skin to the disk or cold clouds

which efficiently reflects low energy photons incident on it. This reflection, together with Comptonization of any intrinsic accretion disk emission, leads to a strong soft X-ray continuum emission, while the ionized skin produces a line spectrum, dominated by oxygen and Fe L complexes (Ross & Fabian 1992, Netzer 1993).

3.2.5 ABSORPTION *Cold material* In hard-X-ray selected samples (e.g. Piccinotti et al 1982) a significant fraction of all AGN exhibit large column densities of cold material in the line of sight [$N(\mathrm{H}) > 10^{22}$ atoms/cm^2]. However, it now has become clear (see Section 3.4 below) that almost all of the objects that show such absorption can be classified as either transition objects between Seyfert I and II galaxies (Seyfert 1.5s), Seyfert IIs, or narrow emission line galaxies. [NELGs, which originally were objects selected on the basis of their hard X-ray emission (Wilson 1979), were subsequently found to have strong narrow emission lines, and are now thought to be strongly related to Seyfert IIs.] Thus the occurrence of absorption by cold matter in "true" Seyfert I galaxies is rather rare.

Ionized material Even with the addition of Compton reflection and its associated Fe K fluorescence line, detailed fits to the 2–20 keV spectra of Seyfert Is showed that an absorption edge due to ionized Fe was often required (Pounds et al 1990, Nandra 1991). Although not well constrained the fitted K-edge energies implied ionization states of ~Fe XX–XXV. Indirect support for the presence of such material came from the detection of a distinct signature of spectral variability (see Section 4.1.3 below). This is the *warm absorber* model, and further support for its relevance has come recently with the detection of absorption due to highly ionized oxygen, in *ROSAT* observations of MCG-6-30-15 (Nandra and Pounds 1992) (Figure 5) and NGC 5548 (Nandra et al 1992).

This additional physical component, by producing a spectral flattening at ~1 keV by oxygen K and Fe L shell absorption can, incidentally, reconcile the spectral index of 1.7 seen in the *EO* SSS results (Petre et al 1984, Reichert et al 1985), with the intrinsic index of 1.9 derived from reflection fits (Section 3.3.3). While the low spectral resolution of past experiments hampers detailed analysis, it seems clear that the extensive moderate quality spectra to be obtained in the next few years will yield much new information on the frequency and nature of absorption features from ionized material in Seyfert Is.

3.3 *Quasars*

We shall use an operational definition of a quasar as an object either of high redshift, $z > 0.1$, and/or of high luminosity $L(\mathrm{x}) > 6 \times 10^{44}$ ergs/sec.

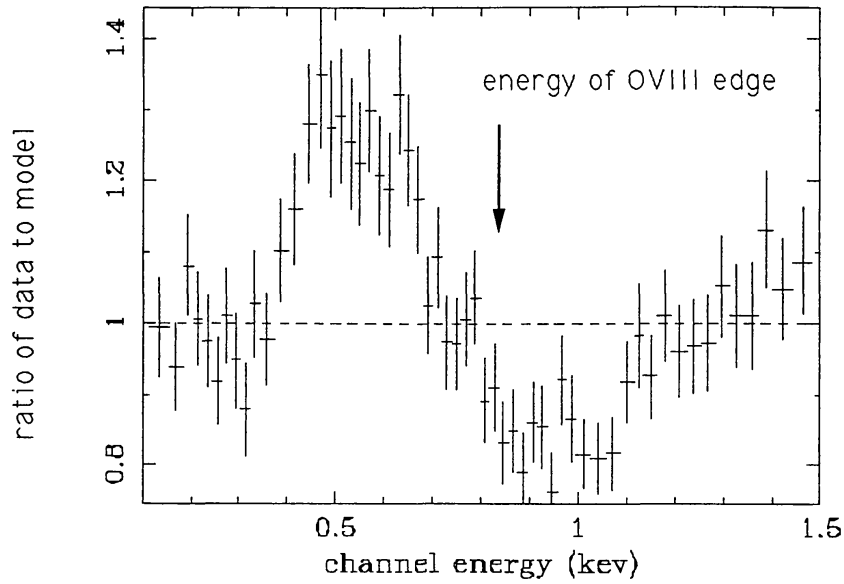

Figure 5 The ratio of the *ROSAT* data to a power-law model for MCG-6-30-15. Note the strong deviation from a power-law model at $E \sim 850$ eV consistent with a deep ionized OVIII edge. (From Nandra et al 1992b.)

3.3.1 CONTINUUM The largest sample of 2–20 keV spectra of quasars are from the *Ginga* satellite (Williams et al 1992) and *EXOSAT* (Comastri et al 1992, Lawson et al 1992). These data are of generally lower statistical quality than those of the (typically brighter) Seyfert Is. In a somewhat unexpected result, given the commonly accepted idea that radio-quiet quasars are simply more luminous versions of Seyfert I galaxies, the quasars with good signal-to-noise have a mean 2–20 keV index, in a simple power-law fit of $\Gamma \sim 2.0$, steeper than that of Seyfert Is. If the one discrepant flat spectrum object, PG 1426-129, is removed from the *Ginga* sample, the mean index is 2.04 ± 0.2, and the *EXOSAT* sample is in good agreement with $\Gamma \sim 1.91 \pm 0.11$. For both samples, the radio-quiet objects have a wider spread of indices than Seyfert Is do. The radio-loud objects appear to be systematically flatter, by $\delta\Gamma \sim 0.2$ in the 2–10 keV band, than the radio quiet objects (Williams et al 1992, Lawson et al 1992) and show a relatively uniform slope of $\sim 1.66 \pm 0.07$ with narrow dispersion.

The $E < 3$ keV spectra of quasars obtained by the *EO* IPC (Wilkes & Elvis 1987) show a variety of spectral slopes, with the radio-loud objects, again, having a systematically flatter spectrum, with $\Gamma \sim 1.5$, than the radio-quiet objects, which have $\Gamma \sim 2$. Recent *ROSAT* results (Brunner et al 1992) find a smaller difference between the radio-loud and radio-quiet objects, with both showing steeper low energy indices, of $\Gamma \sim 2.5$ for radio-

quiet and, $\Gamma \sim 2.2$ for radio-loud quasars, similar to the $\delta\Gamma = 0.2$ found in the 2–20 keV band. It seems likely that the steeper slopes arise from the somewhat softer bandpass of the *ROSAT* PSPC, compared with the *EO* IPC, and that a greater fraction of a soft excess is being detected. In interpreting all such simple power-law fits to low energy data we repeat the cautionary remark that such fits are strongly dependant on the galactic column density and on the existence of any complex spectral structure.

The similarity of the radio-loud 2–20 keV spectral index to the observed index for Seyfert Is seems to be only a superficial resemblance. Detailed spectral analysis shows that the radio-loud objects are not a spectral composite of a steeper power law plus a harder component with iron spectral features, as the *Ginga* spectra show that the radio-loud quasars do not require reflection (Williams et al 1992). Indeed, apart from one low luminosity spectrum of 3C273 (Williams et al 1992, Turner et al 1990) and PHL 1657 (where source confusion is a problem) there are no radio-loud spectra that show significant evidence for any deviations from the simple power-law form in the 2–20 keV energy band (Williams et al 1992).

3.3.2 FE K LINE EMISSION Only the two brightest quasars, 3C273 and 1E1821+653 (Turner et al 1990, Kii et al 1991), show significant Fe line emission, although Mkn 205 (Williams et al 1992) has an Fe line at lower significance. The line in the radio-loud quasar 3C273 is also weak (<50 eV EW) and would not have been seen from the other, fainter radio-loud quasars. The line in 1E1821+643 appears "normal" in EW but the best fit energy, $E \sim 6.7$ keV in the rest frame (Kii et al 1992) is not consistent with most of the Seyfert I galaxies.

3.3.3 REFLECTION The existence of a Compton reflection component in the radio-quiet quasars is uncertain. Significant spectral distortions are seen in all of the *Ginga* sample, but in 4 of the 6 they are better described by a partial covering model than reflection. If this effect is substantiated with a larger sample, it may indicate that the more luminous quasars have less cold material that can produce a reflection hump than the Seyfert Is do. Thus in radio-quiet quasars we may be seeing more of the direct emission, whose spectral slope is similar to that inferred from reflection model fits to the Seyfert Is. Alternatively, the preference for partial covering over reflection may be indicative of additional complexity, possibly due to a warm absorber. Support for this alternative is provided by observations of MR 2251-179 (Halpern 1984, Pan et al 1990), a radio-quiet quasar in which ionized absorbing material is seen. However, the steeper underlying spectral index would then imply a real difference between the emission conditions in the radio-quiet quasars and Seyfert Is.

3.3.4 SOFT EXCESS There is good evidence (Urry et al 1989, Masnou et al 1992, Puchnarewicz et al 1992) that a significant fraction of quasars show a sharp rise in their spectrum to low energies, similar to the soft excess seen in Seyfert Is. As noted by Masnou et al (1992) and Comastri et al (1992), a larger fraction of radio-quiet objects show soft excesses. The form of this soft excess has been difficult to quantify because of the low energy cutoff imposed by our own interstellar medium. However, in at least one object, PG1211, the variability of the soft component rules out bremmstrahlung as an origin (Elvis et al 1986). A power-law description gives Γ ranging from 3.7 to 5.2; the high-energy tail of a blackbody gives temperatures in the range 40–80 eV. The intersection of this soft excess emission with the hard X-ray power law is in the energy interval 0.3–0.75 keV, in the source rest frame (Comastri et al 1992).

The *ROSAT* all-sky survey (RASS) spectral data for optically identified AGN (Brinkman 1992) have been fit to a single power-law form and show a wide dispersion in apparent power-law indices (partly due to poor statistics). However, the trend is for higher z objects to show flatter spectra than lower z objects (Schartel et al 1992). This may indicate that the spectra are composite in a manner consistent with redshifting the soft continuum excess in the spectrum of Seyfert I galaxies, and that the wide range in measured indices is also an artifact of a single power-law fit to a complex spectrum. This can be seen explicitly using data from the *ROSAT* deep surveys, where a two component model fit to the co-added quasar spectra, in three redshift ranges, (Stewart et al 1993) shows a reduction in the contribution of the soft excess as it is progressively redshifted out of the *ROSAT* band (Figure 6). The mean hard power-law spectral index is ~ 2.1, though when the data are split into higher resolution redshift bins this flattens to $\Gamma \sim 1.9$ (Stewart et al 1993). This change in spectral index with redshift bin size is thought to be due to the blackbody not being a good fit to the soft excess when the redshift bins are large, so the mean power law is probably closer to $\Gamma \sim 1.9$ than to 2.1 (Stewart et al 1993). This would then match fairly well with the spectral index of the Seyfert galaxies measured over this energy range (Petre et al 1984, Reichert et al 1985). It also compares well with the intrinsic value of $\Gamma \sim 1.9$ indicated by Compton reflection models for Seyferts, as expected if quasars are scaled up versions of a Seyfert nucleus, as reflection should have a negligible effect in *ROSAT* below redshifts of 2–3. However, at the time of this writing (early 1993) the data are rather uncertain, and the reality of any trend of spectral index with luminosity is an interesting question to address with future, higher quality spectral data.

Only the two brightest quasars (3C273 and 1821+643) have known broadband (0.3–12 keV) spectra of reasonable quality. A simultaneous

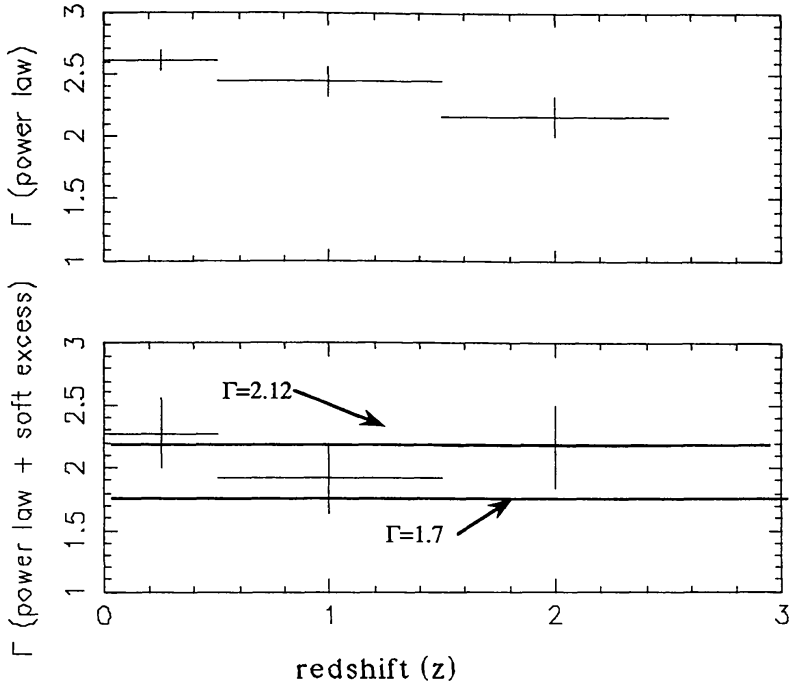

Figure 6 The high energy spectral index, $\Gamma = \alpha + 1$, of *ROSAT* deep survey sources versus redshift (Stewart et al 1993). The top panel shows the results of single power-law fits while the bottom panel shows the fits of a power law with a soft excess. The dotted line shows the mean spectral index of low redshift Seyfert galaxies in the 2–10 keV band. The average *ROSAT* energy corresponds to $\sim 0.8(1+z)$ keV. Beginning at $z \sim 2$ the *ROSAT* energy band starts to overlap the higher energy data.

Ginga-ROSAT observation of 3C273 showed clear evidence for a soft excess, with $kT \sim 200$ eV (Staubert 1992), but this feature was much weaker in a BBXRT observation 10 days later, confirming that the soft excess in this object cannot arise from bremmstrahlung emission (Done et al 1993). The radio-quiet quasar observed simultaneously by *Ginga* and *ROSAT*, 1E1821+643, shows a steepening at $E < 0.5$ keV and a power-law index at higher energies of ~ 1.83—similar to that of Seyfert I galaxies. Clearly more broadband data are needed to resolve the complexities of quasar X-ray spectra.

3.4 *Seyfert IIs*

3.4.1 CONTINUUM FORM AND PHOTOELECTRIC ABSORPTION Although the form of the 2–20 keV continuum of Seyfert IIs is similar to that of Seyfert Is (Kruper et al 1990; Awaki et al 1990, 1991), there are significant differences in the amount of X-ray absorption by cold material. Very few Seyfert I galaxies show significant X-ray absorption by cold material (see Section 3.2.5 above), while, with the singular exception of NGC 1068 (Marshall

et al 1992b, Elvis & Lawrence 1988, Monier & Halpern 1987), all of the X-ray detected Seyfert IIs show evidence for strong absorption by cold material (Awaki et al 1991). Paradoxically, in the unified model (Section 5), the lack of strong absorption in NGC 1068 implies that the actual column density is greater than 10^{24} atoms/cm^2, thus giving it the highest inferred column density of any X-ray Seyfert.

The high column densities seen in Seyfert IIs results in their being significantly fainter soft X-ray sources than Seyfert Is. Although their unabsorbed X-ray luminosity may well be similar to that of the low luminosity Seyfert Is (Awaki et al 1991), there seem to be few intrinsically high luminosity Seyfert IIs (Lawrence 1991, Mulchaey et al 1992, Remillard et al 1993, Awaki et al 1991).

It also appears that narrow line radio galaxies (NLRGs) such as Cen-A, Cyg-A (Arnaud et al 1987), IC5063 (Koyama et al 1992), and 3C109 (Allen & Fabian 1992) show high X-ray column densities and the same spectral indices as Seyfert I galaxies. This is consistent with unification schemes in which the NLRGs and the broad line radio galaxies (such as 3C382 and 3C111) are the radio bright counterparts of Seyfert IIs and Seyfert Is respectively.

3.4.2 FE K LINE EMISSION The majority of X-ray detected Seyfert IIs show extremely strong Fe K lines (Koyama et al 1989, Awaki et al 1990, Marshall et al 1992b), with an EW up to 2 keV in the case of NGC 1068. In the two objects with moderate resolution spectra (BBXRT data for NGC 1068 and Mkn 3) this feature appears complex, with significant emission in both fluorescence and recombination lines (Figure 7). In that analysis each component appears narrow, within the rather limited statistics (Marshall et al 1992a,b). The distribution of EWs in a larger sample of Seyfert IIs observed with *Ginga* is rather broad, overlapping at the lower end with that of Seyfert I galaxies, but extending up to much higher equivalent widths than can be explained in the simple reflection scenario.

Determining whether classical Seyfert IIs show reflection is extremely difficult due to the poor signal-to-noise. However, some NELGs have been shown to require reflection (Matsuoka et al 1990, Bond et al 1992, Nandra 1991), and reflection is suggested in a recent reanalysis of the *Ginga* spectrum of NGC 1068 (Smith et al 1993).

3.4.3 LOW ENERGY COMPONENT The 0.1–3 keV flux in Seyfert IIs is clearly distinct from the heavily absorbed 3–20 keV spectra. The large intrinsic column density detected in the 3–20 keV band would, if it completely covered the central source, completely absorb any intrinsic soft excess such as is seen in Seyfert I galaxies (Awaki 1992). Thus the observed soft component is not a simple continuation of the harder energy data, nor is

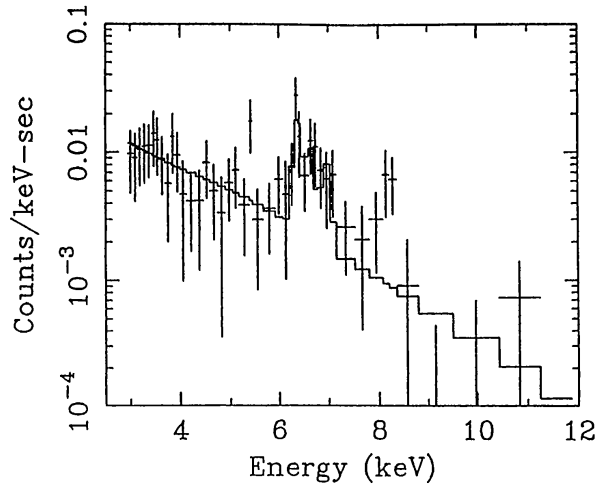

Figure 7 The BBXRT spectrum of the Fe K line region for NGC 1068 (Marshall et al 1992b). The data have been fit with a model (solid line) of 2 Fe K lines at 6.4 keV and 6.67 keV.

it a soft excess such as is seen in Seyfert Is. A currently favored model (see below) has the soft photons being scattered into the line of sight, while the $E > 4$ keV photons come directly to the observer. Lack of time variability in the soft flux (Section 4.3) supports this view.

In NGC 1068, which appears to be an extreme Seyfert II, there is a very strong continuum soft excess, which dominates (Elvis & Lawrence 1988, Marshall et al 1992b) over the hard power law out to ~ 1 keV and appears to be too intense to be due to simple scattering of an intrinsic Seyfert I type of soft excess. However, a substantial contribution to this soft flux is now known to arise from an extended starburst region (Wilson et al 1992), so the true, nuclear, soft component is difficult to quantify.

3.4.4 SOFT X-RAY LINES Iron L lines with an EW > 100 eV at $E \sim 800$–900 eV are also seen in both Seyfert IIs with moderate quality spectra (NGC 1068 and Mkn 3: Marshall et al 1992a). Thus, as for the Fe K lines, soft X-ray line emission may be more prominent in Seyfert IIs than in Seyfert Is. What is unusual is that the expected oxygen absorption feature from warm material (see below) is not present in NGC 1068. While the complex spatial (Wilson et al 1992) and spectral character of this object somewhat hampers interpretation, the lack of such a feature appears robust.

Possible interpretation If the unified models are correct then the central regions of Seyfert IIs are obscured from our direct view by cold material—perhaps the putative molecular torus (Krolik & Begelman 1986). While the torus in NGC 1068—apparently an extreme case—is optically thick

out to at least 20 keV, in many other Seyfert IIs the torus becomes optically thin at ~2–4 keV (Awaki et al 1991). The range of observed columns in Seyfert IIs is too large to be produced by different viewing angles through identical tori, so there must be a range of torus columns in Seyfert IIs (Mulchaey et al 1992). In order to see the broad optical lines in polarized flux (Antonucci & Miller 1985) a scattering cloud of electrons (Miller et al 1991) is required. In this model the scattering region is illuminated by the full nuclear flux, and so becomes strongly ionized (Krolik & Begelman 1986). It therefore produces little low energy absorption but can efficiently scatter low energy X-rays and UV radiation (Kinney et al 1991). It is this scattered flux that is thought to be the origin of the excess soft emission seen in many Seyfert IIs.

The photoionized scattering region will also produce X-ray line emission by fluorescence and recombination (Krolik & Kallman 1987, Band et al 1990). Because the direct continuum is partly or wholly obscured, while the line emitting region is seen directly, the line equivalent width can be substantially enhanced (Krolik & Kallman 1987). This effect is maximized in NGC 1068 where the intrinsic continuum is apparently completely hidden, although some emission may be reflected of the torus wall (Smith et al 1993). The ionized scattering region is also likely to be a source of the iron L line emission (Band et al 1990, but see Smith et al 1993).

Detailed analysis of the X-ray and optical data for NGC 1068 strongly constrains this model. Scattering in the electron cloud can broaden the optical lines by an amount that depends on the temperature of the material. The observed lines are not substantially broadened and so the electron temperature must be relatively low. However, in order to scatter soft X rays, and in particular to not see an oxygen absorption edge, the material must be highly ionized. In this case the electron temperature becomes high (Miller et al 1991, Marshall et al 1992b), conflicting with the optical line widths. It may be that this conflict can be alleviated by allowing for the effects of the spatially extended soft emission in NGC 1068 (Wilson et al 1992).

4. X-RAY TIME VARIABILITY

X-ray emission shows the shortest timescales for AGN variability in any wavelength band (McHardy 1990, Grandi et al 1992). As substantial variability cannot be observed from a source on timescales shorter than the light crossing time of the source (Terrell 1967), then this gives an upper limit to the size of $R < c\delta t$. Assuming a source size of 5 Schwarzschild radii, this can be translated to a limit on the mass of $M < 2 \times 10^6\, \delta t_{100} M_\odot$, where δt_{100} is the variability timescale in units of 100 seconds. The varia-

bility can also be used to derive the efficiency, η, of the source in converting accreting matter to luminosity (Fabian 1979). A change in luminosity δL in time δt implies an efficiency of $\eta = 0.05\, \delta L_{43}/\delta t_{100}$, where $\delta L_{43} = \delta L/10^{43}$. Nuclear processes have a maximum efficiency of $\eta \sim 0.007$; gravitational energy release on accretion gives $\eta = 0.057$ for Schwarzschild or 0.32 for extreme Kerr metrics. Several AGN require efficiencies larger than those produced in nuclear processes, providing the strongest evidence to date that AGN are indeed powered by accretion (Fabian 1992).

4.1 *Continuum Flux Variability in Seyfert Is*

4.1.1 CHAOTIC TOTAL INTENSITY VARIABILITY From the *Ariel-V* sky survey it was already clear that a significant fraction of the Seyfert I and NELGs showed large amplitude ($\delta I/I > 1$) variability on timescales of days (Marshall et al 1981). More sensitive observations found still more rapid variability, on the timescale of hours, for the low luminosity Seyferts NGC 6814 (Tennant & Mushotzky 1983) and NGC 4051 (Marshall et al 1983). However, it was the greatly improved sampling provided by the long and continuous *EXOSAT* observations that first showed that rapid, large amplitude X-ray variability was a common feature of Seyfert galaxies (McHardy 1988, Pounds & McHardy 1988, McHardy 1990).

A recent reanalysis of the *EXOSAT* results (Grandi et al 1992) show that $\sim$40% of AGN, drawn from a hard X-ray selected sample, show variability on a timescale of less than one day. On longer timescales (typically weeks to months) 97% of the same sample showed variability. The short-term variability is most frequently of amplitude $\delta I/I < 1$ and on timescales of much less than one day. In some objects such as NGC 4051 (Figure 8*a*), NGC 6814, and MCG 6-30-15, rapid ($\delta t \ll 6$ hours) large amplitude variability is a very frequent occurrence, while in others such as NGC 4151 (Figure 8*b*) there is very little variability on such short timescales. NGC 6814 is so far unique in showing extreme variability, with a factor of two changes in less than 100 seconds (Tennant et al 1981; Kunieda et al 1990).

There is, perhaps, a subjective difference in the character of the light curves of different AGN. Some, such as Akn 120 (Turner 1988) and NGC 3783 (Grandi et al 1992) seem to show individual events with little variability in between, while others, such as NGC 5506 (a NELG, McHardy & Czerny 1987) show continuous variability. Whether this is an artifact of the rather sparse sampling of some AGN or is a true feature of the variability is unclear.

Power density spectra (PDS) offer one obvious technique to examine the character of the X-ray variability and has been used extensively in the study of X-ray binaries (Van der Klis 1989). When the X-ray light curve

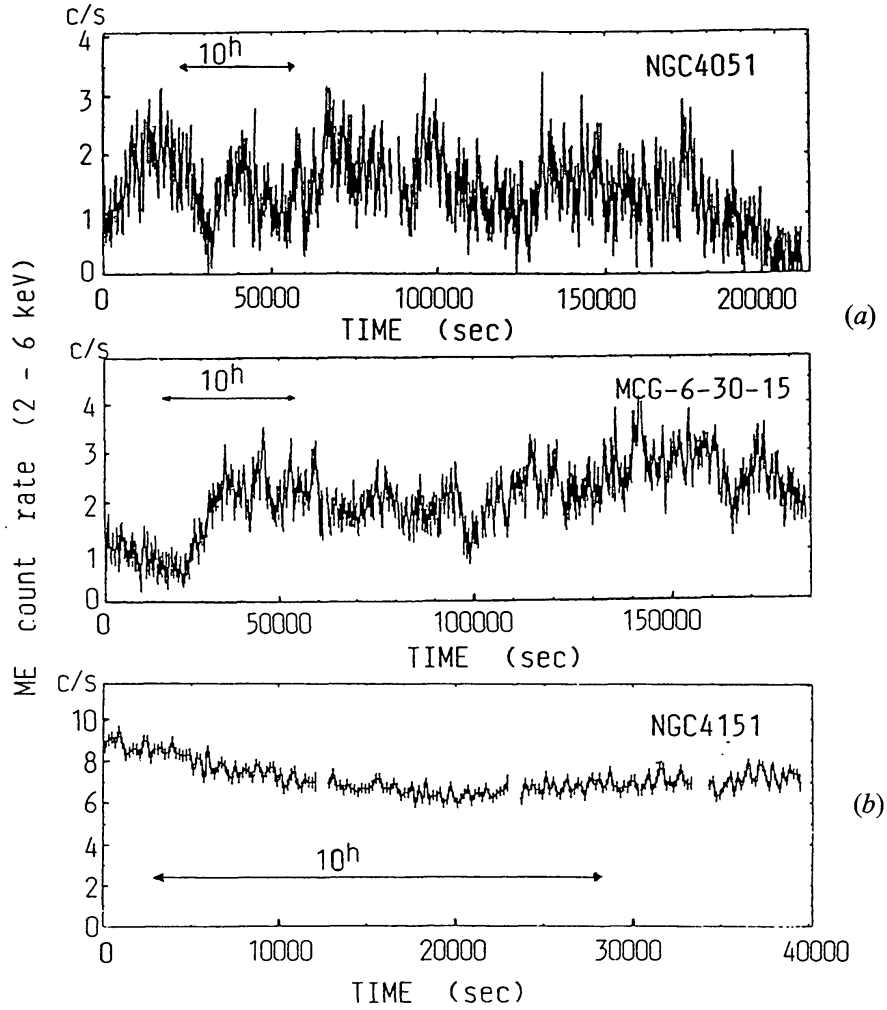

Figure 8 *EXOSAT* 2–10 keV X-ray light curves for NGC 4051, MCG-6-30-15, and NGC 4151. Note that NGC 4051 is varying rapidly during the entire observation on timescales of less than 2000 seconds (McHardy 1990), while NGC 4151 is varying rather slowly having an apparent timescale of >6 hours (Yaqoob 1992).

can be described by a random displacement from a mean value, then the PDS is constant, i.e. has equal power at all frequencies; this is known as a white noise spectrum. A PDS that has more power at low frequencies is called a red noise power spectrum, and can be thought of as the case where a point on the light curve is a random displacement from the adjacent point (rather than the mean).

Over the frequency range from $f = 10^{-3}$ to 10^{-5} Hz most Seyfert Is have a PDS with a mean slope of roughly -1.2 in the 2–10 keV band (McHardy 1988), showing no characteristic timescales (see below). The observed f^{-1} noise is characteristic of many systems in nature, but its origin remains

poorly understood (Press 1978). At the low frequency end, the PDS must eventually turn over, since the amplitude of AGN variations does not keep growing with new observations. Such a turnover has been observed in NGC 5506 (McHardy 1990) (Figure 9). At high frequencies, in the absence of relativistic effects, the fastest variability will be determined by the light crossing time of the smallest emission region, so the power spectrum will steepen beyond this finite limit. However, the *Ginga* observations of NGC 4051 (McHardy 1990) and NGC 6814 (Done et al 1992b)—the most sensitive to date, have extended each PDS down to ~ 300 seconds, with no evidence for high frequency steepening indicative of a characteristic timescale. Thus, in these objects at least, the X-ray emission region must have components with a size scale smaller than $\sim 10^{13}$ cm.

There are strong indications (Barr & Mushotzky 1986, Zamorani et al 1984 McHardy 1988) that more luminous sources have "slower" variability. These authors used different ways of expressing this, either as an increase in the timescale for a source to change by a factor of two ("two-folding timescale") with luminosity (Barr & Mushotzky 1986), or as a scaling of the PDS such that the power at a given frequency decreases with luminosity (McHardy 1990). Of course, if the PDS is a pure power law, the two-folding timescale has no formal meaning (Lawrence et al 1987), and measurement of the change of the PDS with luminosity is more useful.

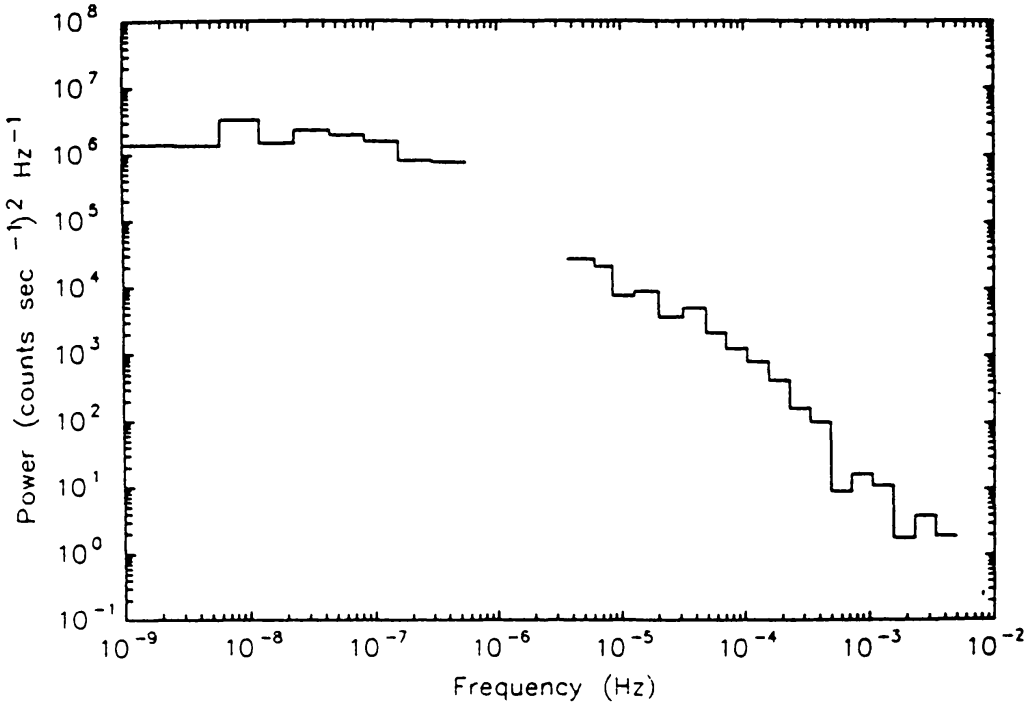

Figure 9 The power density spectrum of NGC 5506 (McHardy 1990) in the 2–10 keV band. Notice the f^{-1} behavior at high frequencies ($> 10^{-5}$ Hz) and the flatter f^0 behavior at low frequncies ($< 10^{-7}$ Hz).

However, to date, few good PDS exist and reliance on the two-folding timescale remains necessary. In practice, this may not be such a bad assumption: There is a linear correlation between the two-folding timescale and measurements of the mass of the central object made via dynamical means, in which the central mass is determined by measuring the velocities of the optical lines and their distance from the central object via photoionization arguments (Wandel & Mushotzky 1986, Padovani & Rafanelli 1988). The fact that these completely different means of estimating the scale of the central object agree, both quantitatively and qualitatively, is an indication that both are likely to be measuring a quantity proportional to the mass of the central object. Clearly, what is needed to quantify ideas about the nature of X-ray variability is a larger sample of objects for which both the power at a fixed timescale and the frequency at which the PDS flattens can be determined.

One problem with Fourier power spectra is that they are meaningful only when the variability is linear. This is not yet known to be the case for AGN and, indeed, in the optical light curves for the OVV quasars there is evidence that the variability is nonlinear (Vio et al 1992)—a perhaps unsurprising result if relativistic beaming dominates in these objects. An alternative method to the use of power spectra is fractal analysis (McHardy & Czerny 1987). This analysis is appropriate only if the AGN variability is governed by a small number of variables rather than being truly stochastic. Recent results from Cyg X-1 (Lochner et al 1989) and some *EXOSAT* AGN (Lehto et al 1992) indicate that this is not the case, and that the X-ray variability is indeed stochastic.

There is as yet no consensus on how the X-ray variability is produced. Presumably long-term variability is caused by changes in the global accretion rate, but the rapid variability cannot arise in this manner as the viscous timescale in the accretion disk is much too long. The lack of physical understanding of the variability means that there is no generally accepted way to describe the fluctuations. The most commonly used method, the so-called shot noise model, assumes that the variability is caused by a superposition of many similar events (Sutherland et al 1978). However, a random distribution of simple impulsive events with exponential decay gives an f^{-2} power spectrum—much steeper than those generally observed. Such models can be made to fit the power spectra by using a range of shot decay times, so that for NGC 4051 the minimum decay time for the individual shots is $\sim$300 seconds (Papadakis & Lawrence 1992). However, this is by no means a unique description of the variability, and the range of decay timescales seems contrived. Another idea for producing the variability is to link the X-ray emission regions with the disk, so that intrinsic variability is amplified by the Doppler rotation

velocities (Abramovicz et al 1991), or produced by disk oscillations (Wallinder 1991). However, at present there is no compelling evidence for any of these models.

In Section 6 we review the most probable X-ray emission mechanisms, and note here that any variability in the mechanism by which the emitting electrons gain energy will lead to a change in the X-ray flux.

4.1.2 PERIODIC VARIABILITY Detection of periodic variability in the continuum offers a unique measure of the size of the emitting region. To date, only one AGN, the low luminosity Seyfert I galaxy NGC 6814, has shown truly "periodic" variability (Figure 10*a*,*b*).It has a period of 12,132 seconds which has remained constant, to within 100 seconds, from 1985 to 1991 (Mittaz & Branduardi-Raymont 1989, Fiore et al 1992a, Done et al 1992b). The extremely rapid variability of this Seyfert (L_x varies by a factor of 2 in 50 seconds, Kunieda et al 1990) appears to be related to the periodic component, which also shows a spectral signature indicative of absorption (Leighly et al 1992, but see Yamauchi et al 1992 for a different view). The sharp transition, if due to an occultation, indicates that most of the flux comes from a region with site less than 100 light seconds. This indicates that the periodic component does not come from the intrinsic emission region, but is due to modulation of the primary X-ray flux by material around the source.

If the period is connected with rotation, as seems likely given the stability of the system, then the secondary object is probably a normal main sequence star, captured by interaction with the accretion disk (Syer et al 1991, Sikora & Begelman 1992, King & Done 1993). The rotation period limits the mass of the black hole as the orbit radius must be larger than the last stable orbit for the black hole. This gives $M < 2 \times 10^7\ M_\odot$ in a Schwarzschild geometry (Mittaz & Branduardi-Raymont 1989). The luminosity of the source sets a lower limit to the mass from the Eddington limit, of $M > 10^5\ M_\odot$. Thus in NGC 6814, if rotation is indeed the correct interpretation of the periodicity, there is at least $10^5\ M_\odot$ in a region smaller than 3×10^{12} cm, again strongly supporting the standard black hole picture of AGN.

To our knowledge no other AGN definitely show periodic emission, although there is a weak indication of such a component in NGC 4151 (Fiore et al 1989). However, if the period scales linearly with the mass of the central object, the implied periods for the more luminous AGN would be rather long, >1 day, and would not have been determinable from present data.

4.1.3 CONTINUUM SPECTRAL VARIABILITY Spectral variability is observed in about half of the well studied Seyferts, with the general trend being for a softening of the 2–10 keV spectra with increasing source intensity (Halpern

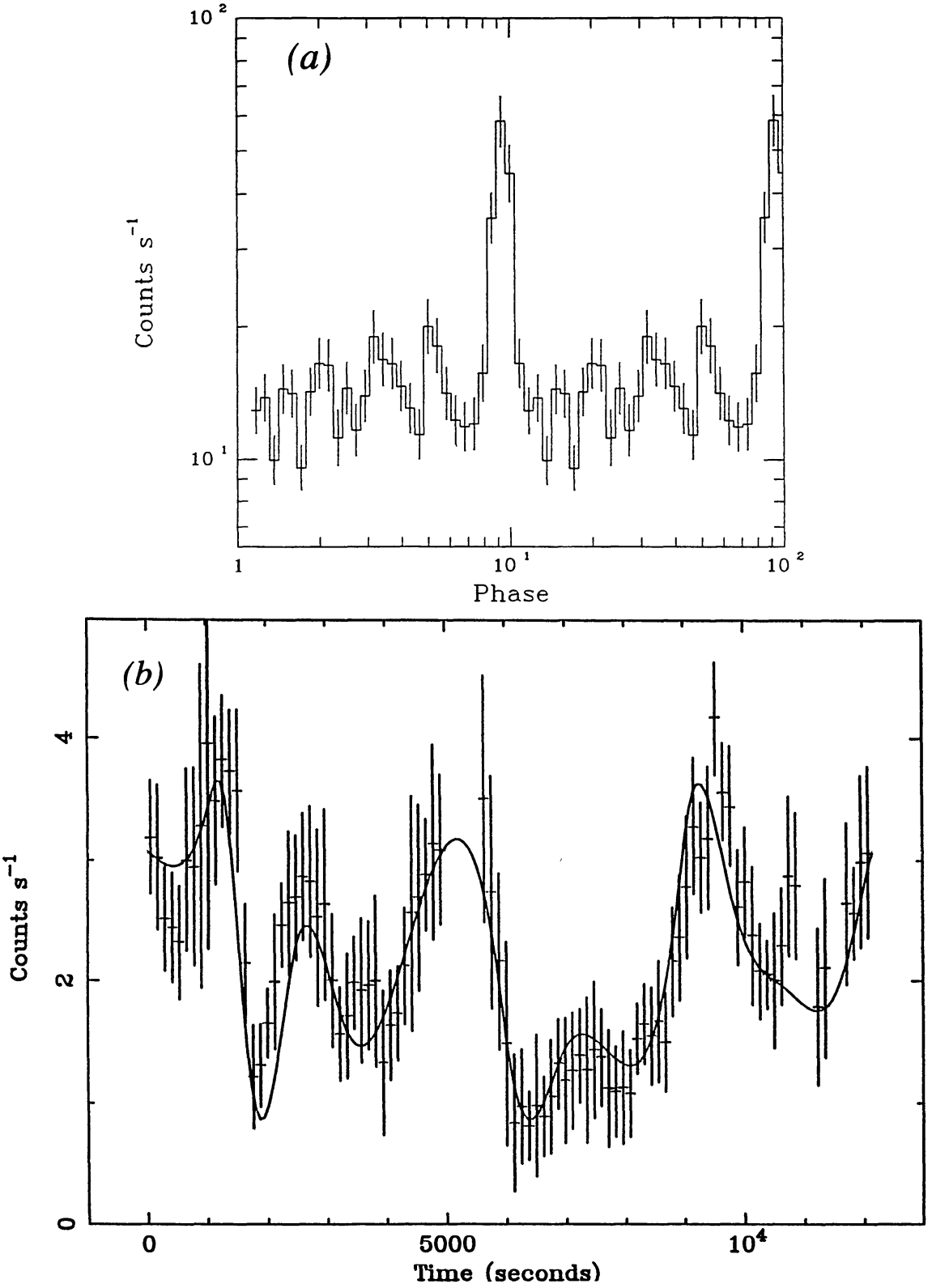

Figure 10 (*a*) *EXOSAT* folded light curve of NGC 6814 in the 2–10 keV band (Fiore et al 1992a). Notice the very simple profile. (*b*) The folded light curve of NGC 6814 in the 5.69–6.84 keV band obtained from *Ginga* observations (Done et al 1992b). Note the complex pulse shape compared to the single peak in the *EXOSAT* folded light curve.

1985, Branduardi-Raymont 1986, Morini et al 1986, Perola et al 1986, Matsuoka et al 1990, Nandra et al 1990, Maraschi et al 1991, Nandra et al 1991, Yaqoob & Warwick 1991, Yaqoob et al 1993, Grandi et al 1992, Kunieda et al 1992, Fiore et al 1992b). There is one clear counter example, NGC 7469, (Barr 1986) in which the power law flattens as the source intensity increases. However, the situation is far from clear as to what is actually varying.

Many observations may be explained by variations in the relative normalizations of the intrinsic and reprocessed spectral components (Section 3) rather than changes in the form of any of them. For example, simple power-law fits to the *EXOSAT* and *Ginga* observations of NGC 5548 show the photon index increasing with hard X-ray flux. When the same data are modeled with a power-law plus reflection component, however, the spectral variability can be entirely accounted for by differential variations of a constant-slope power law and a Compton reflection hump (Nandra et al 1991). Similar behavior has been observed for MCG-6-30-15 (Nandra et al 1990).

There does appear to be unambiguous evidence for variation in the underlying continuum spectrum in at least one Seyfert, NGC 4151 (Perola et al 1986, Yaqoob & Warwick 1991, Yaqoob et al 1993). In this object the effects of reflection and ionized absorption are apparently small (Maisack & Yaqoob 1991, Yaqoob & Warwick 1991, Yaqoob et al 1993), so they do not confuse the interpretation of the spectral variability.

The broadband 0.1–10 keV spectra show complex variations (Grandi et al 1992) which are not easily quantified. This is probably due to the presence of a separate spectral component which dominates at low energy. For example, NGC 5548 (Walter & Courvosier 1990) shows changes in the hard X-ray spectral index which are correlated with variations in the soft to hard X-ray ratio. The variations are in the sense that the 2–10 keV spectrum gets steeper as the ratio of soft to hard flux gets less, while in 3C 120 (Maraschi et al 1991) the 2–10 keV spectrum steepens when the ratio of soft to hard flux increases.

4.1.4 ABSORPTION VARIABILITY Variations in the column density of line-of-sight cold material have been seen in only a few objects: NGC 4151 (Barr et al 1977, Yaqoob & Warwick 1991, Yaqoob et al 1993), ESO 103-G55 (Warwick et al 1988), Centaurus-A (Mushotzky et al 1978a, Morini et al 1989), NGC 6814 (Kunieda et al 1990, Leighly et al 1992), and NGC 5506 (Bond et al 1992). In the unified scheme (see Section 5) large X-ray column densities may be due to the cold torus, the disk of the galaxy itself (Lawrence & Elvis 1982), or perhaps the broad line clouds or material associated with the accretion disk. The apparent rarity of variations in

cold absorption is consistent with all these explanations, although the occurrence of variability at all argues for some component associated with either the broad line clouds or the edge of the accretion disk, since the other two regions are not expected to change on observable timescales. Further constraints on this material can be derived from NGC 4151 (Yaqoob et al 1993) and NGC 5506 (Bond et al 1992) where the column is observed to change and then return to its original value. This may imply a coherent structure rather than any random cloud distribution, and so may support an association with the material located in the disk.

Variability in the apparent ionization state of "warm material" has been claimed in several Seyfert Is: MCG-6-30-15 (Nandra et al 1990), NGC 5548 (Nandra et al 1991), NGC 4051 (Fiore et al 1992b), NGC 6814 (Turner et al 1992) as is seen as an apparent change in the absorbing column or softness ratio as a function of flux. Theoretically, as the flux of the central source increases, the ionization state of the absorber also increases, reducing the opacity of the gas at low energies. In low resolution data this leads to an apparent change in the absorbing column or softness ratio as a function of flux and thus modifies the observed continuum shape. For higher spectral resolution detectors, the warm absorber will modify the continuum in a complex manner, which has strong energy dependence; detailed study of this must await future observations.

4.2 *Line Variability in Seyfert Is*

Variability is the key to understanding the origin of the Fe K line. If it originates from a disk (Section 3.2.3) quite rapid variability may be expected, whereas an origin further from the central source, such as in the broad line region responsible for the broad optical and UV lines (Ferland & Mushotzky 1982), would yield much slower variability.

The *EXOSAT* observations of Cen-A (Morini et al 1989) show very little variation in the flux of the Fe K line, while the continuum varied by a factor of more than two. *Ginga* (Yaqoob & Warwick 1991) and BBXRT observations of NGC 4151 (Weaver et al 1992) also showed very little variation in line flux during large continuum changes. However, these AGN are both special cases, in which large line-of-sight columns of cold gas provide an obvious "external" source for the K-line fluorescence. In NGC 6814, on the other hand (Kunieda et al 1990, Done et al 1992b) the Fe K line tracked the continuum variations with a lag of less than 250 seconds (Figure 11), indicating an origin very close to the central source. NGC 4051 (Fiore et al 1992b) also shows quite rapid variability in its Fe line intensity. These two low luminosity Seyferts hence provide good candidates for the major reprocessing component arising very close to the central power-law source.

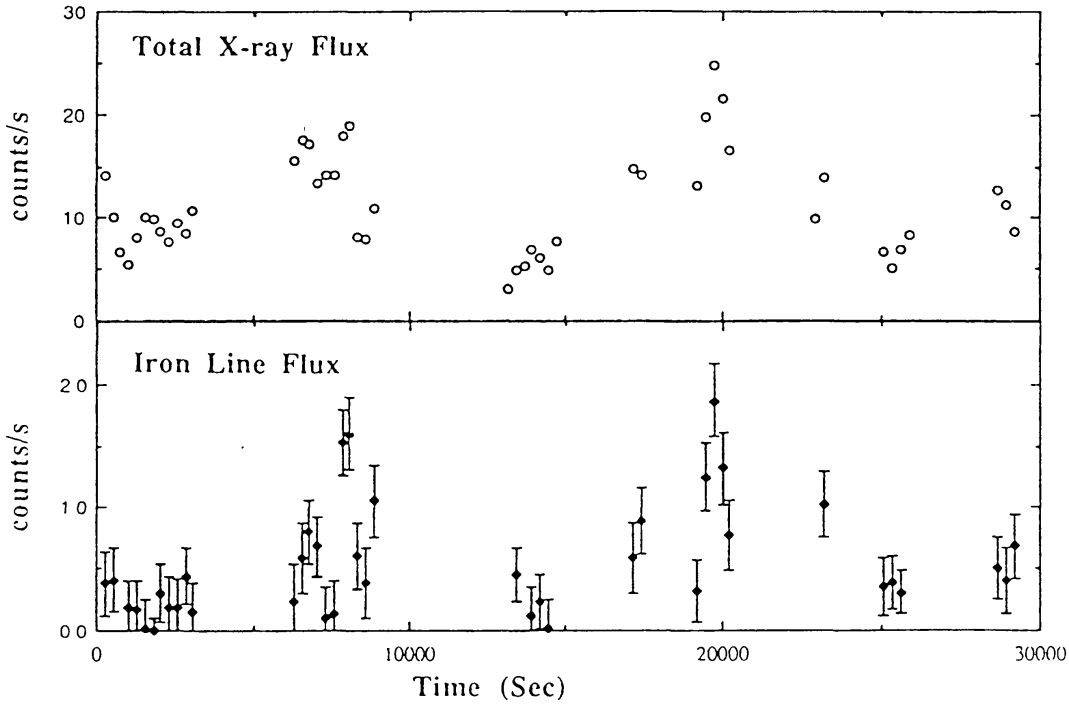

Figure 11 The light curve of the Fe K line and continuum flux in NGC 6814 binned in 250 second intervals (Kunieda et al 1990). Note that there is no lag between the continuum and line variations.

These two different extremes of intensity variability for the Fe K line probably relate to two physically separate sites for its origin. There may be more. We anticipate that when moderate resolution spectra of the Fe lines become available for additional AGN there will be a strong correlation between line profiles and line variability.

There is at present very little information on variability of the low energy spectral features. If the absorption features are due to a dense warm absorber it may be anticipated that they will vary virtually simultaneously (on the order of the recombination time) with the continuum. Time variability data will again be crucial in determining the origin of the emission features: If arising in an accretion disk they could vary relatively rapidly, while if from within the BLR (Broad Line Region) or some other large structure variations will be much slower.

4.3 *Continuum Variability in Seyfert IIs*

The NELGs seem to show the same hard X-ray variability characteristics as the Seyfert Is [cf NGC 5506 (McHardy & Czerny 1987), NGC 7314 (Turner 1987)], as does the Seyfert II, IRAS 1832 (Awaki 1991). This suggests that in all these cases much of the 2–20 keV flux comes directly from the central object and is not scattered radiation. However, as noted

by Wandel & Mushotzky (1986) Seyfert IIs seem to vary more slowly for their dynamical mass than Seyfert Is. This has been interpreted to mean (Mulchaey et al 1992) that their true optical-UV luminosity has been underestimated, in agreement with the unified model.

At soft X-ray energies, the emission is expected to be scattered radiation and thus vary slowly, if at all. This is indeed the case for NGC 1068 (Monier & Halpern 1987). A spectacular example of this sort of energy dependent variability is NGC 4549 (Iwasawa et al 1993) which shows rapid variability at high energy and little if any variability at $E < 5$ keV. However, there is one Seyfert II, Mkn 78 (Urry et al 1986), that shows relatively rapid variability at low energies too.

5. THE BIG PICTURE

Based on the above observational results (as well as others in the radio and optical bands), in recent years a consensus picture of the central regions of radio-quiet AGN has been developed. This is the so-called unified model (for a detailed description see Antonucci 1993). We shall briefly describe this model and the X-ray observations that have refined and supported it. (Figure 12)

At the center of the AGN is a massive black hole (MBH). The non-thermal continuum is thought to originate within 20 Schwarzschild radii of the MBH from an, as yet, unspecified structure. Close in and surrounding the MBH is an optically thick, geometrically thin, accretion disk, identified with the Compton reflector and the origin of the "cold" Fe K line in many objects. In a quasi-spherical volume surrounding the MBH is a cloud of hot electrons and ions, perhaps the warm absorber responsible for low energy spectral features and high ionization Fe features. This material is also the probable origin of the 6.7 keV line in NGC 1068 (and perhaps other Seyfert IIs) as well as being the innermost part of the electron scattering region responsible for the reflection of the Seyfert II continuum. Further out, at several light days for a $L(\mathrm{x}) \sim 10_{43}$ erg/sec Seyfert I galaxy, are the clouds responsible for the broad optical lines and perhaps for the narrow Fe K lines (as in NGC 4151). Still further out is a region of thick [$N(\mathrm{H}) > 10^{23}$ atoms/cm^2) cold material in the shape of a torus. This material obscures the line of sight to the central engine in Seyfert IIs and NELGs and is thought to be responsible for the high X-ray column densities in these objects. Finally, at scales of 100s of pc to kpcs lies the narrow line region responsible for the narrow optical and UV lines in Seyferts of both types and the farthest extensions of the electron scattering cloud. At present, no imprint of the narrow line region has been identified in the $E > 2$ keV X-ray spectrum of an AGN. However, the ultra-soft

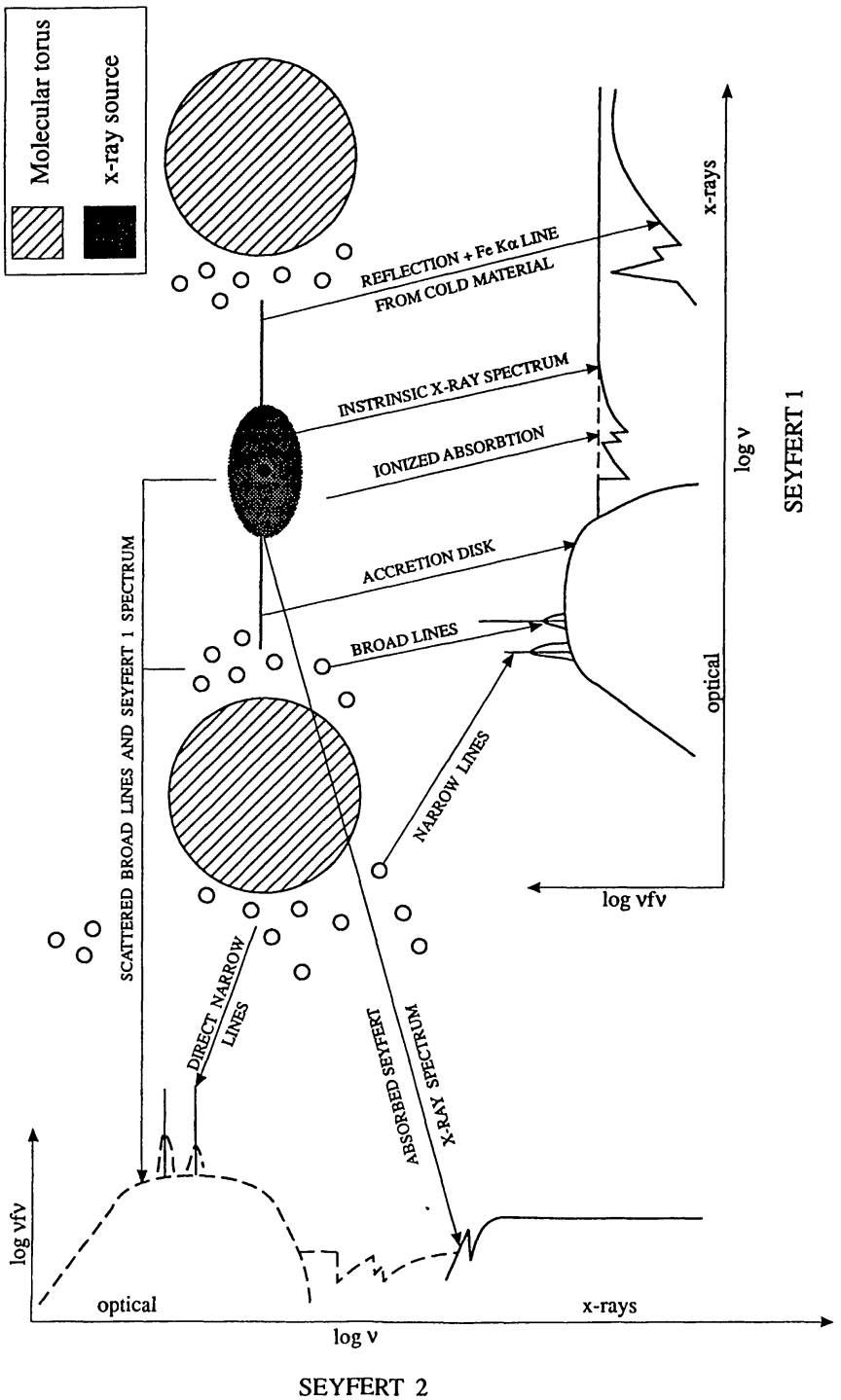

Figure 12 The Big picture. The current consensus for radio-quiet AGN is that the activity is powered by accretion onto a black hole. The X-ray source itselIf is close to the black hole, and illuminates an optically thick, geometrically thin accretion disk giving rise to a Compton reflection spectrum and an iron Kα line. As the reflection albedo is $\leqslant 10\%$, the majority of the X-ray flux incident on the accretion disk is thermalized and reprocessed into UV/soft X-ray emission, enhancing the UV/soft X-ray emission processes in the disk itself. Further out from the nucleus is the Broad Line region, further out still is a thick obscuring torus, and outside that is the Narrow Line emitting material. Filling the "hole" in the torus is a column of highly ionized material, possibly formed by irradiation of the inner edge of the molecular torus. This ionized material is probably the "warm absorber" seen in the spectra of some Seyfert I galaxies.

For lines of sight that intercept the torus, much of the nuclear flux is absorbed. Thus the broad lines, UV spectrum, and soft X-rays cannot be seen directly, leading to a classification of the object as a "less active" Seyfert II. However, some nuclear flux scattered over the top of the torus by the ionized material can be observed, leading to the observation of polarized broad lines, and weak UV and soft X-ray emission. The torus is generally transparent to X rays at energies greater than 4 keV, so that the hard X-ray nuclear flux can be seen directly. The only current known exception to this is NGC 1068, in which even the hard X rays are scattered flux.

continuum component in NGC 4151—found to remain constant over several years (Pounds et al 1986), and extended components in NGC 4151 and NGC 1566 (Elvis et al 1990), may represent emission from the NLR (Narrow Line Region) inter-cloud medium.

6. MODELS OF THE CONTINUUM

As pointed out by Rees (1984), black holes are intrinsically relativistic objects, since the characteristic kinetic energy of a proton is >1 MeV at <1000 Schwarzschild radii. Thus the main theoretical problem in interpreting the X-ray data of AGN is how to tap this relativistic energy and so produce X-rays. Optically thick accretion disks (Shakura & Sunyaev 1973), the "baseline" theoretical structure for AGN, cannot produce hard X-rays and must accordingly be modified. There have been a relatively large number of suggested modifications (for a recent review see Bregman 1990) including: (*a*) a disk instability (Shapiro et al 1976) that results in the innermost regions reaching very high temperatures, (*b*) dissipation of energy into a corona (Haardt & Maraschi 1991), possibly through magnetic reconnection, and (*c*) direct production of relativistic particles by shocks (Kazanas & Ellison 1986), or electromagnetic processes (Blandford & Znajek 1977). However, none of these ideas has received universal support, since most schemes for production of the high energy continuum have had a rather ad hoc basis (Kazanas 1992). Indeed, most models have concentrated on mechanisms of photon production and have tended to ignore how the energy is actually produced. We remind the reader that the photon index Γ is related to the commonly used energy index α by $\Gamma = \alpha + 1$.

6.1 *Theories of the Continuum*

The early indication of a "universal" spectral index in the 2–20 keV band with $\Gamma = 1.7$ stimulated the development of many physical models to explain the nature of the emission. The most robust of these have been thermal (Shapiro et al 1976, Maraschi & Molendi 1991, Sunyaev & Titarchuk 1980, Pozdnyakov et al 1983) and nonthermal Comptonization models (Jones et al 1974) and pair reprocessing models (cf the review by Svensson 1990).

6.1.1 THERMAL COMPTONIZATION In this class of model the X-rays are produced by seed photons scattering off hot electrons with a thermal distribution (cf Pozdnyakov et al 1983). The predicted spectrum is a function of the energy gain of the photon in interaction with the electron. Neglecting down-scattering, the initial and final energy of the photon

can be approximated by $E_f = e^y E_i$, where y is the Compton parameter $\sim(4kT/m_ec^2)\max(\tau, \tau^2)$, τ is the optical depth to Compton scattering, and T is the temperature of the electrons. This gives an approximate power-law spectrum provided $\tau > 0.01$ and $y \ll 10$ up to the thermal rollover at $E \sim kT$–$3kT$ (see Pozdnyakov et al 1983). The analytic power-law spectral index was derived by Sunyaev & Titarchuk (1980) in the special case where the diffusion limit applies ($\tau > 3$) and a good approximation for lower values of τ is given by Zdziarski (1985). The fact that the X-ray spectrum, in general, shows rather small changes in α with large, up to a factor of 10, changes in flux (e.g. Nandra et al 1990, 1991) indicates that, if this model is correct, y must also remain fixed. This sort of fine-tuning can be obtained in models in which the seed photons are produced by reprocessing in material which subtends a large solid angle with respect to the hot electron region (Haardt & Maraschi 1991).

These models also predict (Payne 1980) that the higher energy flux must lag the low energy flux during episodes of strong variability, since higher energy photons are, on average, scattered more often than lower energy ones. The predicted timescales can be rather short (Tennant & Mushotzky 1983), but for the two sources with the best data, NGC 6814 (Done et al 1992a, Leighly et al 1992) and NGC 4051 (Fiore et al 1992b) this effect is not seen. Thus, if Compton scattering is indeed the radiation mechanism, the source must be small.

6.1.2 NONTHERMAL COMPTON MODELS The basic physics of these models is the same as of the thermal models, except that the X-ray power law is produced by the scattering of low energy photons by relativistic particles. For a power-law distribution of particle energies $N(\gamma) \sim \gamma^{-p}$ the resulting spectrum is a power law of index $\alpha = (p-1)/2$ (cf Rybicki & Lightman 1979). These models can reproduce the observed spectra but must assume that the intrinsic relativistic electron distribution is also in a narrow range of allowed parameters. If it is assumed (Kardashev 1962, Rees 1967) that there is a steady state between injection and Compton and synchrotron cooling, the particle spectrum assumes a unique value with $p = 2$ and a slope of $\alpha = 1/2$. Although this circumvents the fine-tuning of the acceleration mechanism, the resultant spectrum is too flat to reproduce the X-ray spectra. Nature has somehow solved this problem in double radio sources (Rothschild et al 1983) where the observed particle spectrum is $p = 2.4$, which gives $\alpha = 0.7$, but whatever mechanism applies here is unlikely to work in the entirely different conditions of electron cooling in the core of AGN.

6.1.3 SYNCHROTRON SELF-COMPTON SCATTERING These models are similar to those above, but instead of the seed photons being produced externally,

the relativistic electrons produce synchrotron photons by scattering virtual magnetic field photons (Jones et al 1974). These synchrotron photons are then the seed photons for the inverse Compton process. Although the Compton spectrum initially has the same spectral index as the synchrotron spectrum, it steepens at higher energies. This mechanism has found favor in the radio-loud objects, in the context of relativistically beamed emission from the jet (e.g. Ghisellini et al 1986) where direct measurement of source sizes and energy densities can be consistent with the observed X-ray fluxes and spectra. However, in radio-quiet objects, the IR-optical bands seem to have quite different variability properties from the X-rays, ruling out synchrotron self-Compton models (Done et al 1990b, but see Celloti et al 1991 for a possible resolution).

6.1.4 PAIR REPROCESSING The rapid variability and high luminosity seen in AGN show them to be compact, in the sense that the X-ray photon density in the source is so high that it is probable that any gamma rays produced cannot escape from the source without interacting with these photons, and so produce an electron-positron pair (for a recent review see Svensson 1992). The probability of this process is determined by the compactness parameter $l = (L/R)\sigma_T/mc^3 = 60\ \tau_{511\,\mathrm{keV}}$, where $\tau_{511\,\mathrm{keV}}$ is the optical depth to pair production for photons at the threshold energy 511 keV. At least 5 Seyfert Is have $l > 60$ (Done & Fabian 1989), when the size is obtained from variability light travel time arguments. As 4 of these 5 are "typical" objects there is reason to suspect that this process is important in most Seyferts.

In thermal Comptonization the introduction of pair reprocessing means that there is a feedback link between the luminosity of the source and its optical depth and temperature (Svensson 1984, Zdziarski 1985). However, the compactness and optical depth of the model must be fine-tuned to obtain $\alpha = 1$. One possible way to avoid such fine-tuning is to assume that the seed photons for the Comptonization are produced from reprocessing (Maraschi & Molendi 1991, Haardt & Maraschi 1991). For an extensive corona over a disk of cold material, the disk intercepts half of the energy of the Comptonizing corona, thermalizing it into the soft photons. The equality of the seed photon and Compton luminosity gives $\alpha = 1$.

Nonthermal Compton scattering of the pairs in the limit of multiple pair generations also gives $\alpha = 1$ naturally (Svensson 1986, Fabian et al 1986, Svensson 1987, Lightman & Zdziarski 1987, Done & Fabian 1989, Done et al 1990a, Zdziarski et al 1990).

Both thermal and nonthermal Compton models seem then to offer the required stable, $\alpha \sim 1$, X-ray spectrum seen in many AGN. Observations from *GRO* will crucially distinguish between these two scenarios through

the very different high energy behaviors of the two models. If the spectrum turns over below $E \sim m_e c^2$ and shows no sign of recovery, this would conflict with the predictions of the nonthermal models and support the thermal models. Conversely, a recovery from the Compton down-scattering break and a strong annihilation line at 511 keV will favor the nonthermal models.

6.2 *The Total Energy Budget*

The broadband spectra of AGN (McDowell et al 1989, Ward et al 1987, Sanders et al 1990) show that the mean spectral index between the X-ray and optical bands [the so-called α(ox)] (Zamorani et al 1981) is 1.25 for Seyfert galaxies and varies as $L(\mathrm{o})^{0.1}$ (Kriss & Canizares 1985, Avni & Tananbaum 1986, Mushotzky & Wandel 1989). More luminous objects such as quasars have a larger value of α(ox) and thus *less* X-ray emission per unit optical luminosity. Typical values of α(ox) are ~ 1.5 for quasars (Avni & Tananbaum 1986). Radio-loud objects (Worrall 1987) have ~ 3 times more 2 keV X-ray flux per optical flux than radio-quiet objects at the same optical luminosity.

In Seyfert I galaxies (Lawrence & Elvis 1982, Ward et al 1987, Edelson & Malkan 1986) the X-ray energy density is comparable to the UV-IR at ~ 6 kev. The broadband 10^{12}–10^{15} Hz spectra can be described by a power law of energy index $\alpha = 1$ (equal energy per decade). Since the observed X-ray spectra are flatter than $\alpha = 1$, they have more energy per unit decade at higher energies. Integrating over 1–20 keV, the band over which the spectra are well observed, shows that for Seyfert galaxies with $L(\mathrm{x}) \sim 10^{43}$ this band has roughly 1/5 as much energy as the 10^{12}–10^{15} Hz (IR-UV)band. At $\log L(\mathrm{x}) \sim 10^{46}$ the X-ray band has $\sim 1/20$ the luminosity of the optical-IR. This relationship shows a factor of 3 variance at all luminosities. However, there is, to our knowledge, no object that is "X-ray quiet" (Avni & Tananbaum 1986).

If one extends the bandpass of integration to 500 keV, the X-ray luminosities would increase by a factor of 2–3, depending on whether the high energy power law (photon number) index is 1.7 or 2. It thus seems likely that the X-ray band carries a significant fraction of the total luminosity of the object. The only other reservoir for much of the energy emitted by the AGN lies in the extreme ultraviolet (EUV) where the "Big Bump" (Malkan & Sargent 1982, Laor & Netzer 1989) is purported to radiate most of its energy.

6.3 *Relationship of X-Ray to Other Wavelength Bands*

The relationship of the X-ray to the other wavelength bands remains unclear at present. Time variability data present a rather complex picture.

For some objects, like NGC 4051 (Done et al 1990b), the optical band shows no variability on timescales of hours or less while the X-ray flux is fluctuating by factors of more than two. On the other hand, in NGC 5548 (Clavel et al 1992), on timescales of days the X-ray and UV fluxes track each other quite closely, with no apparent lag or lead. This has stimulated models in which the UV is produced by reprocessing of the X-ray flux in the accretion disk. In order for these models to work there obviously must be sufficient energy in the X-ray band to provide the observed UV flux. While this depends rather sensitively on the spectrum of the "Big Bump," simple arguments indicate that the X-ray spectra in these objects must extend with a flat $\alpha < 1$ slope to $E > 500$ keV, in order to provide the necessary energy. This then implies that the X-ray-γ-ray band carries most of the radiated energy of the AGN for low luminosity objects. For high luminosity quasars the low ratio of X-ray to optical luminosity indicates that the UV flux cannot, primarily, be reprocessed X-rays (Malkan 1991).

The connection of the IR to the X-rays is unclear. Various authors (Edelson & Malkan 1986, Worrall 1987, Kriss 1988, Mushotzky & Wandel 1989, Carleton et al 1987) find excellent correlations of the X-ray and the IR luminosity in the 1–4 μ band, but Sanders et al (1990), analyzing the PG quasar sample, claim that these correlations are an artifact and find no correlation when just fluxes are considered. In $\sim 1/3$ of radio quiet quasars (Elvis et al 1986) there also seems to be a direct connection, in that a power-law fit to the IR data roughly predicts the 2 keV flux. Since it has now become fashionable, because of the lack of IR variability and the steepening of the spectrum at ~ 1–2 μ (Bregman 1990), to believe that the IR is due to dust reprocessing of UV photons, it is unclear why the IR and the X-ray data would be so closely related unless the initial seed photons for reprocessing are in the X-ray band. However, as indicated above this seems unlikely for quasars.

6.4 *Similarity to Galactic Black Holes*

It now seems clear (McClintock 1992) that there exists a population of stellar mass black holes in our galaxy (Galactic black hole candidates, or GBHC), all discovered as the counterparts to bright X-ray sources. The X-ray spectrum of these objects (White et al 1984), despite the ~ 6 orders of magnitude difference in mass of the central object, bears a remarkable resemblance to those of AGN. The GBHC energy spectra are steep at low energies and flat at high energies. If fitted to a blackbody or thick accretion disk spectrum (Mushotzky 1988, Tanaka 1990) the effective temperature of the low energy emission scales appropriately with the assumed mass of the central object. In addition, the GBHC show the same range of power-law spectral slopes as is seen in AGN, have Fe lines with EW $\sim$ 100 eV,

and display the signature of Compton reflection in their high energy spectrum (Ebisawa 1991, Done et al 1992a).

The time variability characteristics of the Galactic black hole candidates are also similar to AGN with their PDS having the same general form, being flat at low frequencies and steepening to $f^{-1.2}$ at higher frequencies (Miyamoto et al 1992). The observed low frequency break in the PDS of GBHC of $\sim$ few seconds, compared to that in low luminosity AGN of $\sim$ many days, also appears to scale with the ratio of the luminosity of the objects. The overall similarity in the properties of these objects to those of AGN strengthens the association of activity in the nuclei of galaxies with massive black holes. Since the X-ray fluxes of these objects is two to three orders of magnitude larger than that of the brightest AGN and they have been seen to vary 6 orders of magnitude faster, observations of GBHC may well provide a basis for more detailed understanding of their more massive brethren. However, it is entertaining to note (Penston 1986) that if the variability timescales do indeed scale as the mass, then one second of observation of a GBHC is equivalent to one year of observation of a typical Seyfert galaxy!

7. CONCLUSIONS

X-ray spectral and temporal data are now powerful tools for understanding the nature of active galaxies. The X-ray spectra are probes of the innermost regions of AGN and contain the only discrete spectral features thought to arise from close to the central object. The Fe 6.4 keV feature and the Compton reflection "bump" are evidence for the existence of large column densities of cold material close to the central engine. Measurements of the shape of the Fe line hold the promise of determining the mass of the central object and proving the existence of a black hole. The recently discovered X-ray spectral features at lower energies, furthermore, may hold the key to determining the nature of the ionized material close to the central engine. While the combination of rapid variability in the X-ray domain with the large fraction of energy emitted between 0.1–200 keV is the surest evidence for a compact object powering the AGN phenomenon, the lack of temporal signatures in most AGN has not permitted detailed understanding of the cause of variability nor the measurement of a definitive physical scale in these objects.

The origin of the X-ray energy and the power-law shape of the continuum, the most fundamental of the properties of AGN, are still not well understood. There are a variety of likely physical mechanisms that can produce the hard continua. New high energy X-ray data are crucial to resolving this issue. The remarkable similarity between the X-ray spec-

tral and temporal properties of AGN and the Galactic black hole candidates may hold the key to understanding the origin of the continuum and the power-law form of the power density spectrum. X-ray studies of AGN are still at a relatively early and crude stage, but the great increase in observational capability in the 1990s, with *ROSAT*, *ASCA*, *JET-X*, *SAX*, *GRO*, *XMM*, and *AXAF*, promises that the next few years should be extremely productive.

ACKNOWLEDGMENTS

RFM would like to thank T. J. Turner and G. Madejski for useful suggestions and stimulating discussions. He also thanks E. Boldt for providing the research atmosphere in which this paper could be written. CD acknowledges support from an SERC fellowship. We would like to thank G. Stewart for Figure 6 in advance of publication, P. Nandra for Figures 3*a*,*b* and 5, and I. George for Figure 4*b*.

Literature Cited

Abramowicz, M. A., Bao, G., Lanza, A., Zhang, X-H. 1991. *Astron. Astrophys.* 245: 454
Allen, S. W., Fabian, A. C. 1992. *MNRAS* 258: 29p
Antonucci, R. R. J. 1993. *Annu. Rev. Astron. Astrophys.* 31: 473–521
Antonucci, R. R. J., Miller, J. S. 1985. *Ap. J.* 297: 621
Arnaud, K. A., Branduardi-Raymont, G., Culhane, J. L., Fabian, A. C., Hazard, C., et al. 1985. *MNRAS* 217: 105
Arnaud, K. A. Johnstone, R. M., Fabian, A. C., Crawford, C. S,. Nulsen, P. E. J., et al. 1987. *MNRAS* 227: 241
Avni, Y., Tananbaum, H. 1986. *Ap. J.* 305: 83
Awaki, H. 1991. PhD thesis. Nagoya Univ.
Awaki, H. 1992. In *Ginga Memorial Symp.*, ed. F. Makino, F. Nagase, p. 63. Tokyo: Inst. Space Aeronaut. Sci.
Awaki, H., Koyama, K., Inoue, H., Halpern, J. P. 1991. *Publ. Astron. Soc. Jpn.* 43: 195
Awaki, H., Koyama, K., Kunieda, H., Tawara, Y. 1990. *Nature* 346: 544
Baity, W. A., Rothschild, R. E., Lingenfelter, R. E., Stein, W. A., Nolan, P. L., et al. 1981. *Ap. J.* 244: 429
Baity, W. A., Mushotzky, R. F., Worrall, D., Rothschild, R. E., Tennant, A. F., Primini, F. 1984. *Ap. J.* 279: 555
Band, D. L., Klein, R. I., Castor, J. I., Nash, J. K. 1990. *Ap. J.* 362: 90
Barr, P. 1986. *MNRAS* 223: 29p
Barr, P., Mushotzky, R. F. 1986. *Nature* 320: 421
Barr, P, White, N. E. Sanford, P. Ives, J. C. 1977. *MNRAS* 181: 43p
Bechtold, J., Czerny, B., Elvis, M., Fabbiano, G., Green, R. F. 1987. *Ap. J.* 314: 699
Blandford, R. D., Rees, M. J. 1992. See Holt et al 1992, p. 3
Blandford, R. D., Znajek, R. 1977. *MNRAS* 179: 433
Bond, I., Matsuoka, M., Yamauchi, M. 1992. *Ap. J.* 405: 179
Bowyer, S., Lampton, M., Mack, J. 1970. *Ap. J. Lett.* 161: L1
Boyle, B., Grffiths, R., Shanks, T., Stewart, G., Georgantopoulos, I. 1992. *MNRAS* 260: 49
Bradt, H. V. D., Ohashi, T., Pounds, K. A. 1992. *Annu. Rev. Astron. Astrophys.* 30: 391
Branduardi-Raymont, G. 1986. In *The Physics of Accretion onto Compact Objects*, ed. K. O. Mason, M. G. Watson, N. E. White, p. 407. Berlin: Springer-Verlag
Bregman, J. 1990. *Astron. Astrophys. Rev.* 2: 125
Brinkman, W. 1992. See Brinkman & Trümper 1992, p. 143
Brinkman, W., Trümper, J., eds. 1992. *X-Ray and UV Emission from Active Galactic Nuclei.* Munich: MPE Rep. 184
Brunner, H., Friedrich, P., Zimmermann, H-U., Staubert, R. 1992. See Brinkman & Trümper, p. 198
Carleton, N. P., Elvis, M., Fabbiano, G., Willner, S. P., Lawrence, A. Ward, M. 1987. *Ap. J.* 318: 515

Celloti, A., Ghisellini, G., Fabian, A. C. 1991. *MNRAS* 251: 529
Charles, P. A., Longair, M. S., Sanford, P. W. 1975. *MNRAS* 170: 17p
Clavel, J., Nandra, K., Makino, F., Pounds, K. A., Reichert, G. A., et al. 1992. *Ap. J.* 393: 113
Collin-Souffrin, S. 1992. See Holt et al 1992, p. 119
Comastri, A., Setti, G., Zamorani, G., Elvis M., Giommi, P., et al. 1992. *Ap. J.* 384: 62
Cooke, B., Ricketts, M. J., Maccacaro, T., Pye, J. P., Elvis, M., et al. 1978. *MNRAS* 182: 489
Czerny, B., Elvis, M. 1987. *Ap. J.* 321: 305
Danese, L., DeZotti, G., Fasano, G., Franceschini, A. 1986. *Astron. Astrophys.* 161: 1
Davidson, P. J. N., Culhane, J. L., Mitchell, R. J., Fabian, A. C. 1975. *Ap. J. Letts.* 196: L23
Done, C., Fabian, A. C. 1989. *MNRAS* 240: 81
Done, C., Ghisellini, G., Fabian, A. C. 1990a. *MNRAS* 245: 1
Done, C., Madejski, G. M., Mushotzky, R. F., Turner, T. J., Koyama, K., Kunieda, H. 1992b. *Ap. J.* 400: 138
Done, C., Mulchaey, J. S., Mushotzky, R. F., Arnaud, K. A. 1992a. *Ap. J.* 395: 275
Done, C., Ward, M. J., Fabian, A. C., Kunieda, H., Tsuruta, S., et al 1990b. *MNRAS* 243: 713
Done, C., et al. 1993. In preparation
Ebisawa, K. 1991. PhD thesis. Univ. Tokyo
Edelson, R. A., Malkan, M. A. 1986. *Ap. J.* 308: 59
Elvis, M., Czerny, G., Wilkes, B. J. 1987. In *Physics of Accretion onto Compact Objects*, ed. K. O. Mason, M. G. Watson, N. E. White, p. 389. Berlin: Springer-Verlag
Elvis, M., Fassnacht, C., Wilson A. S., Briel, U. 1990. *Ap. J.* 361: 459
Elvis, M., Green, R. F., Bechtold, J., Schmidt, M., Neugebauer, G., et al. 1986. *Ap. J.* 310: 291
Elvis, M., Lawrence, A. 1988. *Ap. J.* 331: 161
Elvis, M., Maccacaro, T., Wilson, A. S., Ward, M. J., Penston, M. V., et al. 1978. *MNRAS* 183: 129
Fabian, A. C. 1979. *Proc. R. Soc. London Ser. A* 336: 449
Fabian, A. C. 1992. See Tanaka & Koyama 1992, p. 603
Fabian, A. C., Blandford, R. D., Guilbert, P. W., Phinney, E. S., Cueller, L. 1986. *MNRAS* 221: 931
Fabian, A. C., Rees, M. J., Stella, L., White, N. E. 1989. *MNRAS* 238: 729
Ferland, G. J., Mushotzky, R. F. 1982. *Ap. J.* 262: 564
Ferland, G. J., Rees, M. J. 1988. *Ap. J.* 332: 141
Fiore, F., Massaro, E., Barone, P. 1992a. *Astron. Astrophys.* 261: 405
Fiore, F., Massaro, E., Perola, G., Piro, L. 1989. *Ap. J.* 347: 171
Fiore, F., Perola, G. C., Matsuoka, M., Yamauchi, M., Piro, L. 1992b. *Astron. Astrophys.* 262: 37
George, I. M., Fabian, A. C. 1991. *MNRAS* 249: 352
Giacconi, R., Murray, S., Gursky, H., Kellogg, E., Schreier, E., et al. 1974. *Ap. J. Suppl.* 27: 37
Ghisellini, G., Maraschi, L., Tanzi, E. G., Treves, A. 1986. *Ap. J.* 310: 317
Grandi, P., Tagliaferri, G., Giommi, P., Barr, P., Paslumbo, G. 1992. *Ap. J. Suppl.* 82: 93
Guilbert, P. W., Rees, M. J. 1988. *MNRAS* 233: 475
Guilbert, P. W., Fabian, A. C., Rees, M. J. 1983. *MNRAS* 205: 593
Haardt, F., Maraschi, L. 1991. *Ap. J. Lett.* 380: L51
Halpern, J. P. 1982. PhD thesis. Harvard Univ.
Halpern, J. P. 1984. *Ap. J.* 281: 90
Halpern, J. P. 1985. *Ap. J.* 290: 130
Holt, S. S., McCray, R. 1982. *Annu. Rev. Astron. Astrophys.* 20: 323
Holt, S. S., Mushotzky, R. F., Becker, R. H., Boldt, E. A., Serlemitsos, P. J., et al 1980. *Ap. J.* 241: L13
Holt, S. S., Neff, S. G., Urry, C. M., eds. 1992. *Testing the AGN Paradigm.* New York: Am. Inst. Phys.
Inoue, H. 1990. In *Proc. 23rd ESLAB Symp.*, ed. J. Hunt, B. Battrick, p. 783. Paris: Eur. Space Agency
Inoue, H. 1992. In *Proc. of the Laredo Workshop on the Diffuse X-ray Background*, ed. X. Barcons, A. C. Fabian, p. 286. Cambridge: Cambridge Univ. Press
Ives, J., Sanford, P., Penston, M. 1976. *Ap. J. Lett.* 207: L159
Iwasawa, K., et al. 1993. *Ap. J.* 409: 155
Jones, T., O'Dell, S., Stein, W. 1974. *Ap. J.* 188: 353
Jourdain, E., Bassani, L., Bouchet, L., Mandrou, P., Ballet, J., et al. 1992. *Astron. Astrophys. Lett.* 256: L38
Kaastra, J. S., Kunieda, H., Awaki, H. 1991. *Astron. Astrophys.* 1242: 27
Kardashev, N. S. 1962. *Sov. Astron. AJ* 6: 317
Kazanas, D. 1992. See Holt et al 1992, p. 301
Kazanas, D., Ellison, D. C. 1986. *Ap. J.* 304: 178
Kii, T., Makino, F., Otani, C., Ohashi, T., Tashiro, M., et al. 1992. See Tanaka & Koyama 1992, p. 577
Kii, T., Williams, O. R., Ohashi, T., Awaki, H., Hayashida, K., et al. 1991. *Ap. J.* 367: 455

Kinney, A. L., Antonucci, R. R. J., Ward, M. J., Wilson, A. S., Whittle, M. 1991. *Ap. J.* 377: 100
Koyama, K., Awaki, H., Iwasawa, K., Ward, M. 1992. *Ap. J. Lett.* 399: L129
Koyama, K., Inoue, H., Takano, S., Tanaka, Y., Ohashi, T., Matsuoka, M. 1989. *Publ. Astron. Soc. Jpn.* 41: 731
Kriss, G. A. 1988. *Ap. J.* 324: 809
Kriss, G. A., Canizares, C. 1985. *Ap. J.* 297: 177
Krolik, J. H., Begelman, M. 1986. *Ap. J. Lett.* 308: L55
Krolik, J. H., Kallman, T. R. 1987. *Ap. J. Lett.* 320: L5
Krolik, J. H., Kallman, T. R., Fabian, A. C., Rees, M. J. 1985. *Ap. J.* 295: 104
Kruper, J., Urry, C. M., Canizares, C. R. 1990. *Ap. J. Suppl.* 74: 347
Kunieda, H., Hayakawa, S., Tawara, Y., Koyama, K., Tsuruta, S., Leighly, K. 1992. *Ap. J.* 384: 482
Kunieda, H., Turner, T. J., Awaki, H., Koyama, K., Mushotzky, R. F., Tsusaka, Y. 1990. *Nature* 345: 786
Laor, A. 1990. *MNRAS* 246: 369
Laor, A. 1991. *Ap. J.* 376: 90
Laor, A., Netzer, H. 1989. *MNRAS* 238: 897
Lawrence, A. 1987. *Publ. Astron. Soc. Pac.* 99: 309
Lawrence, A. 1991. *MNRAS* 252: 586
Lawrence, A., Elvis, M. 1982. *Ap. J.* 256: 410
Lawrence, A., Pounds, K. A., Watson, M. G., Elvis, M. 1987. *Nature* 325: 692
Lawrence, A., Watson, M. G., Pounds, K. A., Elvis, M. 1985. *MNRAS* 217: 685
Lawson, A. J., Turner, M. J. L., Williams, O. R., Stewart, G. C., Saxton, R. 1992. *MNRAS* 259: 743
Leighly, K., Kunieda, H., Tsuruta, S. 1992. See Holt et al 1992, p. 93
Lehto, H. J., Czerny, B., McHardy, I. 1992. *MNRAS* 261: 125
Lightman, A. P., White, T. R. 1988. *Ap. J.* 335: 57
Lightman, A. P., Zdziarski, A. A. 1987. *Ap. J.* 319: 643
Lochner, J. C., Swank, J. H., Szymkowiak, A. E. 1989. *Ap. J.* 337: 823
Maisack, M., Kendziorra, E., Mony, B., Staubert, R., Dobereiner, S., et al. 1992. *Astron. Astrophys.* 262: 433
Maisack, M., Yaqoob, T. 1991. *Astron. Astrophys.* 249: 25
Makishima, K. 1986. In *The Physics of Accretion onto Compact Objects*, ed. K. O. Mason, M. G. Watson, N. E. White, p. 249. Berlin: Springer-Verlag
Malkan, M. A. 1991. In *Structure and Emission Properties of Accretion Disks*, ed. C. Bertout, S. Collin, J.-P. Lasota, J. Tran Thanh Van, p. 165. Gif sur Yvette: Ed. Frontiers
Malkan, M. A., Sargent, W. L. 1982. *Ap. J.* 254: 22
Maraschi, L., Chiappetti, L., Falomo, R., Garilli, B., Malkan, M., et al. 1991. *Ap. J.* 368: 138
Maraschi, L., Molendi, S. 1991. *Ap. J.* 353: 452
Marshall, F. E., Boldt, E. A., Holt, S. S., Jahoda, K. M., Kellet, R. L., et al. 1992a. See Tanaka & Koyama 1992, p. 233
Marshall, F. E., Holt, S. S., Mushotzky, R. F., Becker, R. 1983. *Ap. J. Lett.* 269: L31
Marshall, F. E., Netzer, H., Arnaud, K., Boldt, E. A., Holt, S. S., et al. 1992b. *Ap. J.* 405: 168
Marshall, N., Warwick, R. S., Pounds, K. A. 1981. *MNRAS* 194: 987
Masnou, J., Wilkes, B. J., Elvis, M., McDowell, J. M., Arnaud, K. A. 1992. *Astron. Astrophys.* 253: 5
Matsuoka, M., Yamauchi, M., Piro, L., Murakami, T. 1990. *Ap. J.* 361: 440
Matt, G., Perola, G. C., Piro, L. 1991. *Astron. Astrophys.* 247: 27
Matt, G., Perola, G. C., Piro, L., Stella, L. 1992. *Astron. Astrophys.* 257: 63 (Erratum in 263: 453)
McClintock, J. 1992. See Tanaka & Koyama 1992, p. 333
McHardy, I. M. 1988. *Mem. Soc. Astron. Ital.* 59: 239
McHardy, I. M. 1990. In *Proc. 23rd ESLAB Symp.*, ed. J. Hunt, B. Battrick, p. 1111. Paris: Eur. Space Agency
McHardy, I. M., Czerny, B. 1987. *Nature* 325: 696
McDowell, J. C., Elvis, M., Wilkes, B. J., Willner, S. P., Oey, M. S., et al. 1989. *Ap. J. Lett.* 345: L13
Miller, J. S., Goodrich, R. W., Mathews, W. G. 1991. *Ap. J.* 378: 47
Mittaz, J. P. D., Branduardi-Raymont, G. 1989. *MNRAS* 238: 1029
Miyamoto, S., Kitamoto, S., Iga, S., Negoro, H., Terada, K. 1992. *Ap. J. Lett.* 391: L21
Monier, R., Halpern, J. P. 1987. *Ap. J. Lett.* 315: L17
Morini, M., Anselmo, F., Molteni, D. 1989. *Ap. J.* 347: 750
Morini, M., Chiappetti, L., Maccagni, D., Maraschi, L., Moltini, D., et al. 1986. *Ap. J.* 307: 486
Mulchaey, J. S., Mushotzky, R. F., Weaver, K. A. 1992. *Ap. J. Lett.* 390: L69
Mushotzky, R. F. 1982. *Ap. J.* 256: 92
Mushotzky, R. F. 1984. *Adv. Space Res.* 3: 10
Mushotzky, R. F. 1988. In *Supermassive Black Holes*, ed. M. Kafatos, p. 143. Cambridge: Cambridge Univ. Press
Mushotzky, R. F. 1991. In *High Energy Astrophysics*, ed. W. Lewin., G. Clark, R. Sunyaev, p. 297. Washington, DC: Natl. Acad.

Mushotzky, R. F. 1992. In *Ginga Memorial Symp.*, ed. F. Makino, F. Nagase, p. 139. Tokyo: Inst. Space Aeronaut. Sci.
Mushotzky, R. F., Baity, W. A, Wheaton, W. A., Peterson, L. E. 1976. *Ap. J. Lett.* 206: L45
Mushotzky, R. F., Holt, S. S., Serlemitsos, P. J. 1978b. *Ap. J. Lett.* 225: L115
Mushotzky, R. F., Marshall, F. E., Boldt, E. A., Holt, S. S., Serlemitsos, P. J. 1980. *Ap. J.* 235: 377
Mushotzky, R. F., Serlemitsos, P. J., Becker, R. H., Boldt, E. A., Holt, S. S. 1978a. *Ap. J.* 220: 790
Mushotzky, R. F., Wandel, A. 1989. *Ap. J.* 339: 674
Nandra, K. 1991. PhD thesis. Univ. Leicester, England
Nandra, K., Fabian, A. C., George, I. M., Branduardi-Raymont, G., Lawrence, A., et al. 1992. *MNRAS* 260: 504
Nandra, K., Pounds, K. A. 1992. *Nature* 359: 215
Nandra, K., Pounds, K. A., Stewart, G. C. 1990. *MNRAS* 242: 660
Nandra, K., Pounds, K. A., Stewart, G. C., George, I. M., Hayashida, K., et al. 1991. *MNRAS* 248: 760
Netzer, H. 1993. *Ap. J.* In press
Ohashi, T., Tashiro, M., Makishima, K., Kii, T., Makino, F., et al. 1992. *Ap. J.* 398: 87
Osterbrock, D., Mathews, W. G. 1986. *Annu. Rev. Astron. Astrophys.* 24: 171
Padovani, P., Rafanelli, P. 1988. *Astron. Astrophys.* 205: 53
Padovani, P., Urry, C. M. 1992. *Ap. J.* 387: 449
Pan, H. C., Stewart, G. C., Pounds, K. A. 1990. *MNRAS* 242: 177
Papadakis, I. E., Lawrence, A. 1992. In *X-ray Emission from Active Galactic Nulcei and the X-ray Background*, ed. W. Brinkmann, J. Trümper, p. 91. Munuch: MPE Rep. 235
Payne, D. 1980. *Ap. J.* 237: 951
Penston, M. 1986. In *The Physics of Accretion onto Compact Objects*, ed. K. O. Mason, M. G. Watson, N. E. White, p. 331. Berlin: Springer-Verlag
Perola, G. C., Piro, L., Altamore, A., Fiore, F., Boksenberg, A., et al. 1986. *Ap. J.* 306: 508
Petre, R., Mushotzky, R. F., Krolik, J. H., Holt, S. S. 1984. *Ap. J.* 280: 499
Piccinotti, G., Mushotzky, R. F., Boldt, E. A., Holt, S. S., Marshall, F. E., et al 1982. *Ap. J.* 253: 485
Piro, L., Yamauchi, M., Matsuoka, M. 1990. *Ap. J. Lett.* 360: L35
Piro, L., Matsuoka, M., Yamauchi, M. 1991. In *Frontiers in X-Ray Astronomy*, ed. Y. Tanaka, K. Koyama, p. 527. Tokyo: Universal Acad.
Pounds, K. A. 1990. *MNRAS* 242: 20p
Pounds, K. A., McHardy, I. M. 1988. In *Physics of Neutron Stars and Black Holes*, ed. Y. Tanaka, p. 285. Tokyo: Universal Acad.
Pounds, K. A., Nandra, K., Stewart, G. C., Leighly, K. 1989. *MNRAS* 240: 769
Pounds, K. A., Nandra, K., Stewart, G. C., George, I. M., Fabian, A. C. 1990. *Nature* 344: 132
Pounds, K. A., Turner, T. J., Warwick, R. S. 1986. *MNRAS* 221: 7p
Pounds, K. A., et al. 1993. In preparation
Pozdnyakov, L. A., Sobol, I. M., Sunyaev, R. A. 1983. *Astrophys. Space Phys. Rev.* 2: 189
Press, W. H. 1978. *Comments Astrophys.* 7: 103
Primini, F. A., Cooke, B. A., Dobson, C. A., Howe, S. K., Scheepmaker, A., et al. 1979. *Nature* 278: 234
Puchnarewicz, E. M., Mason, K. O., Cordova, F. A., Kartje, J., Branduardi-Raymont, G., et al. 1992. *MNRAS* 256: 589
Rees, M. J. 1967. *MNRAS* 137: 429
Rees, M. J. 1984. *Annu. Rev. Astron. Astrophys.* 22: 471
Reichert, G. A., Mushotzky, R. F., Petre, R., Holt, S. S. 1985. *Ap. J.* 296: 69
Remillard, R., et al. 1993. In preparation
Ross, R. R., Fabian, A. C. 1992. *MNRAS* 261: 74
Ross, R. R., Fabian, A. C., Mineshige, S. 1992. *MNRAS* 258: 189
Rothschild, R. E., Mushotzky, R. F., Baity, W. A., Gruber, D., Matteson, J., Peterson, L. E. 1983. *Ap. J.* 269: 423
Rybicki, G. B., Lightman, A. P. 1979. *Radiative Processes in Astrophysics*. New York: Wiley
Sanders, D. B., Phinney, E. S., Neugebauer, G., Soifer, B. T., Matthews, K. 1990. *Ap. J.* 357: 291
Schartel, N., Fink, H., Brinkmann, W., Trümper, J. 1992. See Brinkman & Trümper 1992, p. 195.
Schmidt, M., Green, R. 1983. *Ap. J.* 269: 352
Seyfert, C. K. 1943. *Ap. J.* 97: 28
Shakura, N. I., Sunyaev, R. A. 1973. *Astron. Astrophys.* 24: 337
Shanks, T., Georgantopoulos, I., Stewart, G. C., Pounds, K. A., Boyle, B. J., Griffiths, R. E. 1991. *Nature* 353: 315
Shapiro, S. L., Lightman, A. P., Eardley, D. M. 1976. *Ap. J.* 204: 187
Sikora, M., Begelman, M. C. 1992. *Nature* 356: 224
Singh, K. P., Garmire, G. P., Nousek, J. 1985. *Ap. J.* 297: 633
Sivron, R., Tsuruta, S. 1993. *Ap. J.* 402: 420

Smith, D. A., Done, C., Pounds, K. A. 1993. *MNRAS*. In press
Stark, J. P., Davidson, P. J. N., Culhane, L. 1977. *MNRAS* 174: 35
Staubert, R. 1992. See Brinkman & Trümper, p. 42
Stewart, G. C., et al. 1993. In preparation
Sun, W. H., Malkan, M. A. 1989. *Ap. J.* 346: 68
Sunyaev, R. A., Titarchuk, L. G. 1980. *Astron. Astrophys.* 86: 121
Sutherland, P. G., Weisskopf, M. C., Kahn, S. M. 1978. *Ap. J.* 219: 1029
Svensson, R. 1982. *Ap. J.* 258: 335
Svenson, R. 1986. In *Radiation Hydrodynamics in Stars and Compact Objects*, ed. D. Mihalas, K. H.-A. Winkler, p. 325. Berlin: Springer-Verlag
Svensson, R. 1987. *MNRAS* 227: 403
Svensson, R. 1990. In *Physical Processes in Hot Cosmic Plasmas*, p. 357, ed. W. Brinkmann, A. C. Fabian, F. Giovannelli, p. 357. Dordrecht: Kluwer
Svensson, R. 1992. See Brinkman & Trümper, p. 103
Syer, D., Clarke, C. J., Rees, M. J. 1991. *MNRAS* 205: 505
Tanaka, Y. 1990. In *Proc. 23rd ESLAB Symp.*, ed. J. Hunt, B. Battrick, p. 3. Paris: Eur. Space Agency
Tanaka, Y., Koyama, K., eds. 1992. *Frontiers of Astrophysics*. Tokyo: Universal Acad.
Tananbaum, H., Avni, Y., Branduardi, G., Elvis, M., Fabbiano, G., et al. 1979. *Ap. J. Lett.* 234: L9
Tennant, A. F., Mushotzky, R. F. 1983. *Ap. J.* 264: 92
Tennant, A. F., Mushotzky, R. F., Boldt, E. A., Swank, J. H. 1981. *Ap. J.* 251: 15
Terrell, J. 1967. *Ap. J.* 147: 827
Trümper, J. 1990. *Phys. Bull.* 46: 137
Tucker, W., Kellogg, E., Gursky, H., Giacconi, R., Tanabaum, H. 1973. *Ap. J.* 180: 715
Turner, M. J. L., Williams, O. R., Courvoisier, T. J-L., Stewart, G. C., Nandra, K., et al. 1990. *MNRAS* 244: 310
Turner, T. J. 1987. *MNRAS* 226: 9p
Turner, T. J. 1988. PhD thesis, Leicester Univ., England
Turner, T. J., Done, C., Mushotzky, R. F., Madejski, G., Kunieda, H. 1992. *Ap. J.* 391: 102
Turner, T. J., Pounds, K. A. 1988. *MNRAS* 232: 463
Turner, T. J., Pounds, K. A. 1989. *MNRAS* 240: 833
Turner, T. J., Nandra, K., Jahoda, K., Madejski, G. M., Marshall, F. E., et al. 1993a. *Ap. J.* 407: 556
Turner, T. J., Weaver, K. A., Mushotzky, R. F., Holt, S. S., Madejski, G. M. 1991. *Ap. J.* 381: 85
Turner, T. J., George, I., Mushotzky, R. F. 1993b. *Ap. J.* In press
Urry, C. M., Arnaud, K., Edelson, R. A., Kruper, J. S., Mushotzky, R. F. 1990. In *Proc. 23rd ESLAB Symp.*, ed. J. Hunt, B. Battrick, p. 789. Paris: Eur. Space Agency
Urry, C. M., Kruper, J. S., Canizares, C. R., Rohan, M. L., Oberhardt, M. R. 1986. In *Variability of Galactic and Extragalactic Sources*, ed. A. Treves. Milano: A. A. D. A.
van der Klis, M. 1989. In *Timing Neutron Stars*, ed. H. Ogelman, E. van den Heuvel, p. 27. Dordrecht: Reidel
Vio, R., Cristiani, S., Lessi, O., Provenzale, A. 1992. *Ap. J.* 391: 518
Wallinder, F. 1991. *MNRAS* 253: 184
Walter, R., Courvoisier, T. J. 1990. *Astron. Astrophys.* 233: 40
Wandel, A., Mushotzky, R. 1986. *Ap. J. Lett.* 301: L61
Wandel, A., Petrosian, V. 1988. *Ap. J. Lett.* 329: L11
Ward, M. J., Elvis, M., Fabbiano, G., Carleton, N. P., Willner, S. P. Lawrence, A. 1987. *Ap. J.* 315: 74
Warwick, R. S., Pounds, K. A., Turner, T. J. 1988. *MNRAS* 231: 1145
Weaver, K. A., Mushotzky, R. F., Arnaud, K. A., Serlemitsos, P. J., Marshall, F. E., et al. 1992. *Ap. J. Lett.* 401: L11
White, N. E., Fabian, A. C., Mushotzky, R. F. 1984. *Astron. Astrophys.* 133: L9
Wilkes, B. J., Elvis, M. 1987. *Ap. J.* 323: 243
Wilson, A. S. 1979. *Proc. R. Soc. London Ser. A* 366: 461
Wilson, A. S., Elvis, M., Lawrence, A., Bland-Hawthorn, J. 1992. *Ap. J. Lett.* 391: L75
Winkler, P., White, A. 1975. *Ap. J. Lett.* 199: L139
Williams, O. R., Turner, M. J. L, Stewart, G. C., Saxton, R. D., Ohashi, T., et al. 1992. *Ap. J.* 389: 157
Worrall, D., Giommi, P., Tananbaum, H., Zamorani, G. 1987. *Ap. J.* 313: 596
Yamauchi, M., Matsuoka, M., Kawai, N., Yoshida, A. 1992. *Ap. J.* 395: 453
Yaqoob, T. 1992. *MNRAS* 258: 198
Yaqoob, T., Warwick, R. S. 1991. *MNRAS* 248: 773
Yaqoob, T., Warwick, R. S., Makino, F., Otani, Y., Sokoloski, J. 1993. *MNRAS* 262: 435
Zamorani, G., Henry, J. P., Maccacaro, T., Tananbaum, H., Soltan, A., et al. 1981. *Ap. J.* 245: 357
Zamorani, G., Giommi, P., Maccacaro, T., Tananbaum, H. 1984. *Ap. J.* 278: 28
Zdziarski, A. A. 1985. *Ap. J.* 289: 514
Zdziarski, A. A., Ghisellini, G., George, I. M, Svensson, R., Fabian, A. C., Done, C. 1990. *Ap. J. Lett.* 363: L1